Transfer maps for accelerator modeling

Demin Zhou

Accelerator theory group, Accelerator laboratory, KEK

Acknowledgments

J. Tang, K. Oide, D. Sagan, E. Forest, K. Ohmi

Accelerator physics seminar, Nov. 3, 2023, USTC, Hefei, China

Outline

- References
- Introduction
- Practical examples
- From transfer maps to nonlinear analysis
- Summary

References

- Books
  - General textbooks: A. Chao, S.Y. Lee, A. Wolski, …
  - A. Dragt: Lie methods (2726 pages!)
  - E. Forest: Beam dynamics, Tracking to analysis
- Manuals/Notes on accelerator modeling codes
  - SAD manual, Bmad manual, MAD-X manual
  - Maps used in SAD
- Relevant codes
  - PTC(E. Forest), Bmad(D. Sagan), SAD(K. Oide), MAD-X(CERN team), LEGO(Y. Cai), …
  - PTC is called through interfaces in Bmad and MAD-X

- For future accelerator projects (especially colliders), managing codes for design/simulations is an important task
  - Managing a code team in labs/universities is a challenging task
  - A nice review by D. Sagan et al., “Simulations of future particle accelerators: issues and mitigations”.

	Single Particle Dynamics	Spin Tracking	Taylor Maps	Weak-Strong Beam-Beam Interaction	Electromagnetic Field Tracking	Higher Energy Collective Effects	Synchrotron Radiation Tracking	Wakefields	Extensible	Notes
Bmad (contains PTC) [10]	Yes	Yes	Yes	Yes	Yes	Yes	Yes	Yes	Yes	Reproduces PTC's unique beam line structures. Also simulates X-rays.
MAD8 and MAD-X (includes PTC) [14]	Yes	No	Yes	Yes	No	No	Yes	No	No	
MAD-NG [14]	Yes	No	Yes	Yes	No	No	Yes	No	Yes	Very extensible, embeds LuaJIT
PTC[22]	Yes	Yes	Yes	Yes	Yes	No	No	No	Yes	
SAD [23]	Yes	No	No	Yes	No	Yes	Yes	Yes	No	
SixTrack [25]	Yes	No	Yes	Yes	No	No	No	No	No	Can run on BOINC
Accelerator Toolbox (AT),[6]	Yes	Yes[7]	No	No	No	Yes	No	No	Yes	
ASTRA[8]	Yes	No	No	No	Yes	Yes	No	Yes	No	For space-charge effects evaluation
BDSIM[9]	Yes	No	No	No	Yes	No	No	No	Yes	For particle-matter interaction studies.
COSY INFINITY [11]	Yes	Yes	Yes	No	Yes	No	No	No	No	
DYNAC [12]	Yes	No	No	No	No	No	No	No	No	
Elegant [13]	Yes	No	No	No	Yes	Yes	No	Yes	No	
MERLIN++ [15][16]	Yes	Yes	No	No	No	No	No	Yes	Yes	Other: beam-matter interactions, sliced-macroparticle tracking
OCELOT [17]	Yes	No	No	No	No	Yes	Yes	Yes	Yes	
OPA [18]	Yes	No	No	No	No	No	No	No	No	
OPAL[19]	Yes	No	Yes	No	Yes	Yes	No	Yes	Yes	Open source, runs on the laptop and on x 10k cores.
PLACET[20]	Yes	No	No	No	No	Yes	Yes	Yes	Yes	Simulates a LINAC including wakefields.
Propaga[21]	Yes	No	No	No	No	No	No	No	Yes	
SAMM [24]	Yes	Yes	No	No	No	No	No	No	No	
Zgoubi [26][27]	Yes	Yes	No	No	Yes	No	Yes	No	Yes	Open source.

From Wikipedia

Introduction

- Coordinates and coordinate systems for accelerators
  - Global coordinate system (GCS): Useful for alignments of accelerator components (some codes choose this system for simulations, such as GPT code)
  - Local coordinate system (LCS) (Curvilinear coordinate system): Useful for accelerator physics (optics design, tracking simulations, etc.). Most accelerator codes work with this system
- Design orbit and closed orbit
  - LCS follows the design orbit
  - The ideal particle follows the closed orbit
- Transfer maps
  - Tracking simulations refers to the design orbit
  - Twiss functions and nonlinear analysis refer to the closed orbit $\vec{X}_0$

$$\vec{X}_2 = \mathscr{M}^t_{1\to 2}\vec{X}_1 \qquad \vec{X}_0 = \mathscr{M}^t_{1\to 2}\vec{X}_0$$

$$\vec{X}_1 = \vec{x}_1 + \vec{X}_0, \quad \vec{X}_2 = \vec{x}_2 + \vec{X}_0$$

$$\vec{x}_2 = \mathscr{M}^e_{1\to 2}\vec{x}_1$$

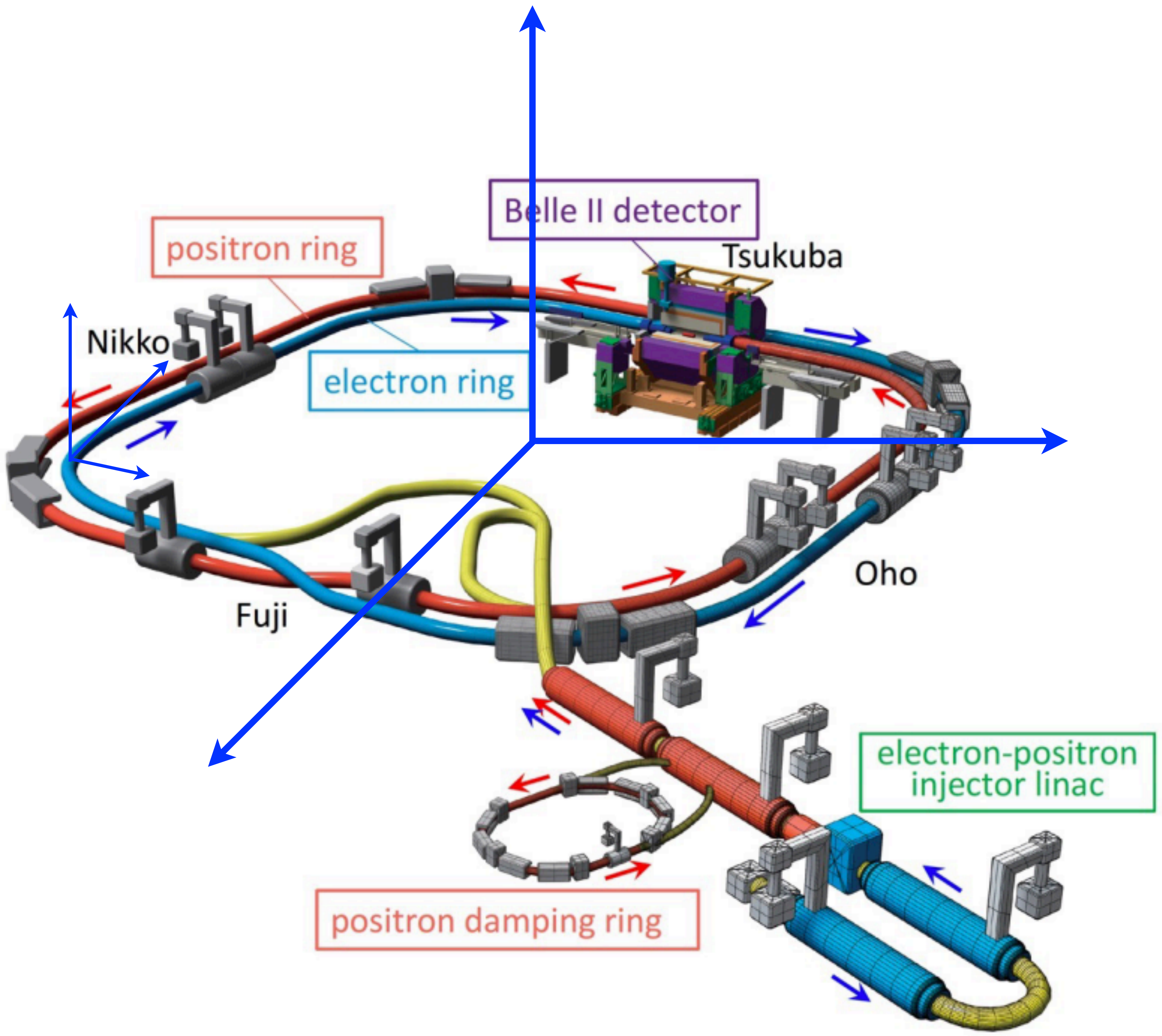

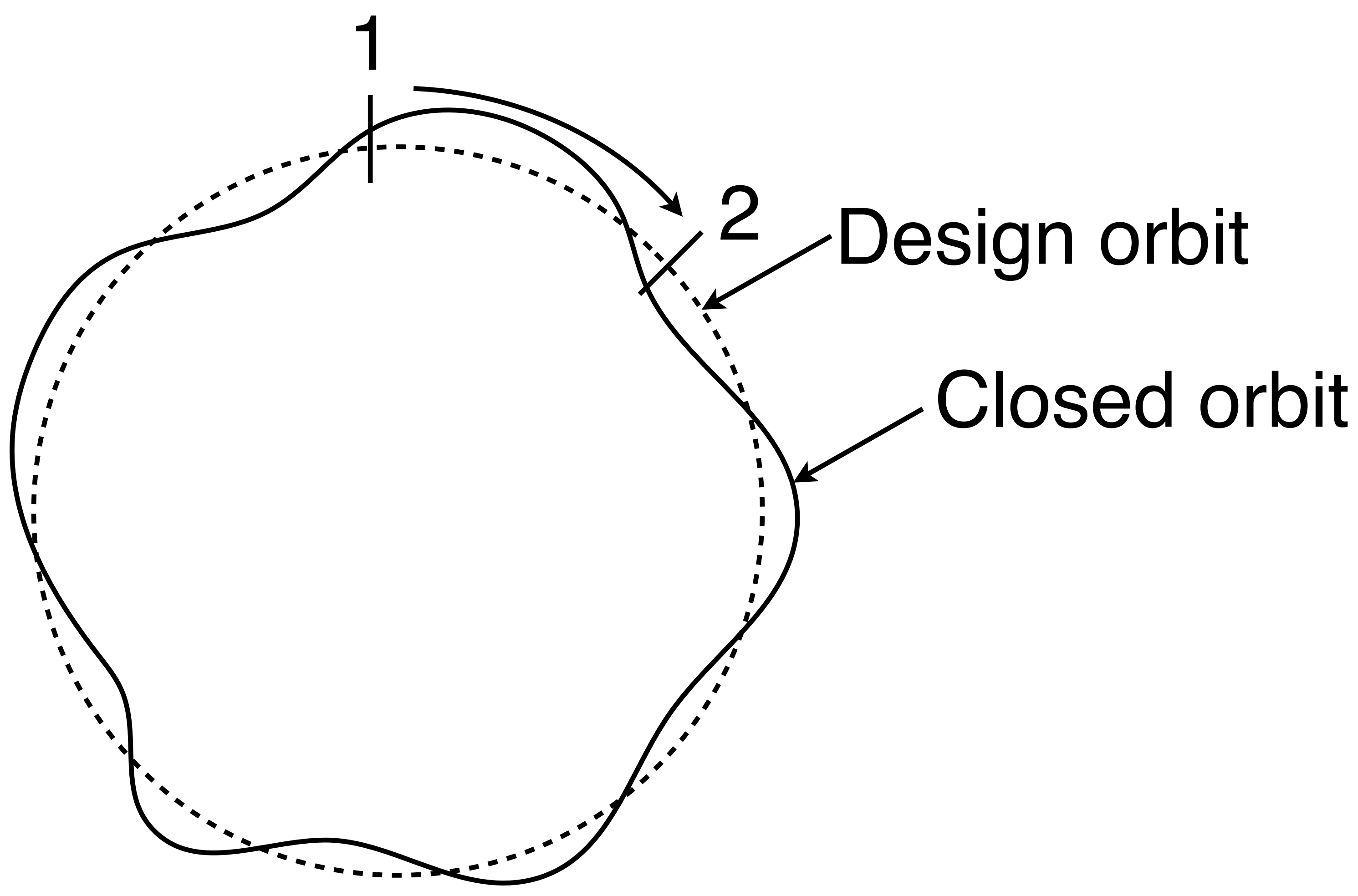

Introduction

- A full description of particle motion along a beam line requires powerful mathematical techniques.
- Suppose the particle's coordinates $(x, p_x, y, p_y, z, \delta)$, the linear transfer map from position 1 to position 2 can be described by the transfer matrix:

$$\begin{pmatrix} x \\ px \\ y \\ p_y \\ z \\ \delta \end{pmatrix}_2 = \begin{pmatrix} R_{11} & R_{12} & R_{13} & R_{14} & R_{15} & R_{16} \\ R_{21} & R_{22} & R_{23} & R_{24} & R_{25} & R_{26} \\ R_{31} & R_{32} & R_{33} & R_{34} & R_{35} & R_{36} \\ R_{41} & R_{42} & R_{43} & R_{44} & R_{45} & R_{46} \\ R_{51} & R_{52} & R_{53} & R_{54} & R_{55} & R_{56} \\ R_{61} & R_{62} & R_{63} & R_{64} & R_{65} & R_{66} \end{pmatrix} \begin{pmatrix} x \\ px \\ y \\ p_y \\ z \\ \delta \end{pmatrix}_1$$

- Note that the transfer matrix around the design orbit is not necessarily the same as around the closed orbit.
- Higher-order nonlinear components (such as sextupoles, octupoles, harmonic cavities, etc.) are often intentionally introduced to control particle motion in a realistic accelerator. But, unwanted nonlinear fields (or nonlinear kicks) often appear in most beam line elements.
- The analysis of nonlinear dynamics relies on tools such as Hamilton's equations and Lie algebra methods. The transfer matrix for linear motion is then extended to the transfer map for nonlinear motion:

$$\overrightarrow{X}_f = \mathscr{M}\overrightarrow{X}_i$$

- The transfer map around the design orbit is not necessarily the same as around the closed orbit

Introduction

- SAD vs. PTC vs. LEGO
  - SAD has a transfer map $\mathscr{M}_i^t$ (=equations of motion) around LCS for each element i-type and a hand-derived linear map $\mathscr{M}_i^e$ (from $\mathscr{M}_i^t$) coded for emittance/Twiss calculations. SAD has no nonlinear map $\mathscr{M}_i^e$ for nonlinear analysis.
  - PTC has a transfer map $\mathscr{M}_i^t$ (=equations of motion) around LCS for each element i-type. PTC dynamically computes $\mathscr{M}_i^e$ from $\mathscr{M}_i^t$. PTC's $\mathscr{M}_i^t$ are similar to SAD's, making the lattice translation between them trivial. PTC tracks particles and "tracks" maps (Polymorphic tracking based on differential algebra technique). PTC does not treat Hamiltonian, though Hamiltonian is frequently discussed in PTC-related publications.
  - LEGO is a code based on Hamiltonian [1]. The tracking maps $\mathscr{M}_i^t$ are derived from Hamiltonian for each element i-type.
- Equations of motion vs. Hamiltonian
  - There are systems where the equations of motion can be found, but a Hamiltonian cannot. These systems are known as non-integrable systems.
  - The existence of a Hamiltonian does not guarantee that a system is integrable. Integrable systems are a class whose equations of motion can be solved analytically. Hamiltonian systems are a more general class of integrable and non-integrable systems.

	SAD	PTC	LEGO
Tracking (Macro particles)	Yes	Yes	Yes
Linear analysis (Twiss/Emittance)	Yes	Yes	Yes
Nonlinear analysis (Taylor maps, RDTs)	No	Yes	Yes
Linear optimization (Twiss/Emittance)	Yes	No	No(?)
Nonlinear optimization (DA/lifetime)	Yes	No	Yes(?)
Spin	Yes	Yes	No

Introduction

- A circular collider presents most of the complexities in accelerator physics. Understanding the transfer maps is essential.
- Transfer maps for single-particle dynamics
  - DRIFT, BEND, QUAD, SEXT, OCT, DECA, MULT, SOL, RF, Wiggler, Aperture(Collimator), …
- Transfer maps for collective effects (not covered in this talk)
  - Beam-beam, Impedances, Space charge, Electron cloud, Ion cloud, ISR, CSR, IBS, Touschek, …
- Full tracking or analysis
  - Analysis of maps using perturbation techniques

$$\mathscr{M} = \mathscr{M}_n \circ \mathscr{M}_{n-1} \cdots \circ \mathscr{M}_i \circ \cdots \mathscr{M}_1 \approx e^{:F_m:} \cdots e^{:F_i:} \cdots e^{:F_3:} e^{:F_2:}$$

  - Analysis of tracking data (Poincare map, FMA, etc.)

$$\vec{X}_f = \mathscr{M} \vec{X}_i$$

  - Perturbation maps used for tracking simulations

$$\vec{X}_f \approx e^{:F_m:} \cdots e^{:F_3:} e^{:F_2:} \vec{X}_i$$

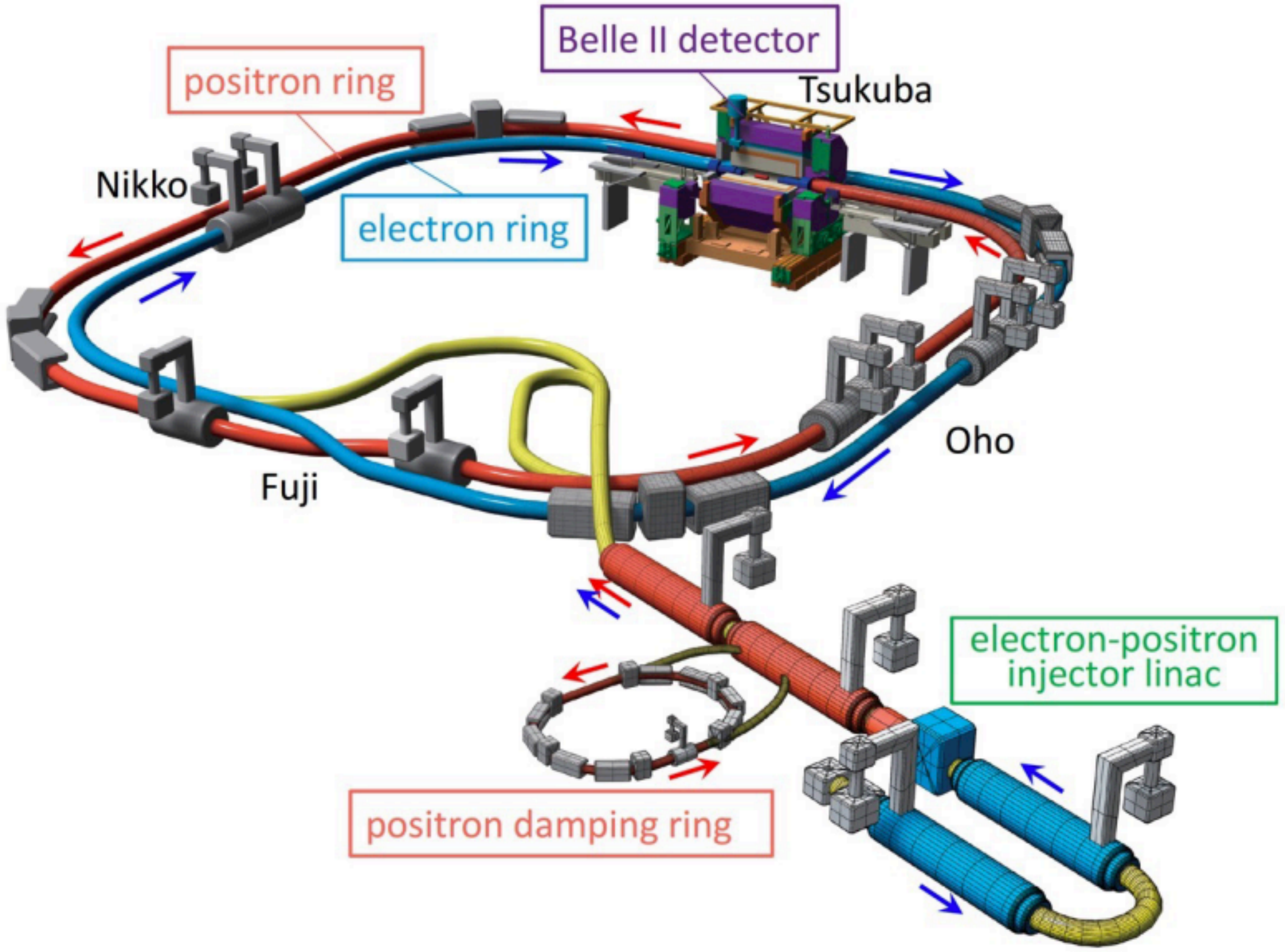

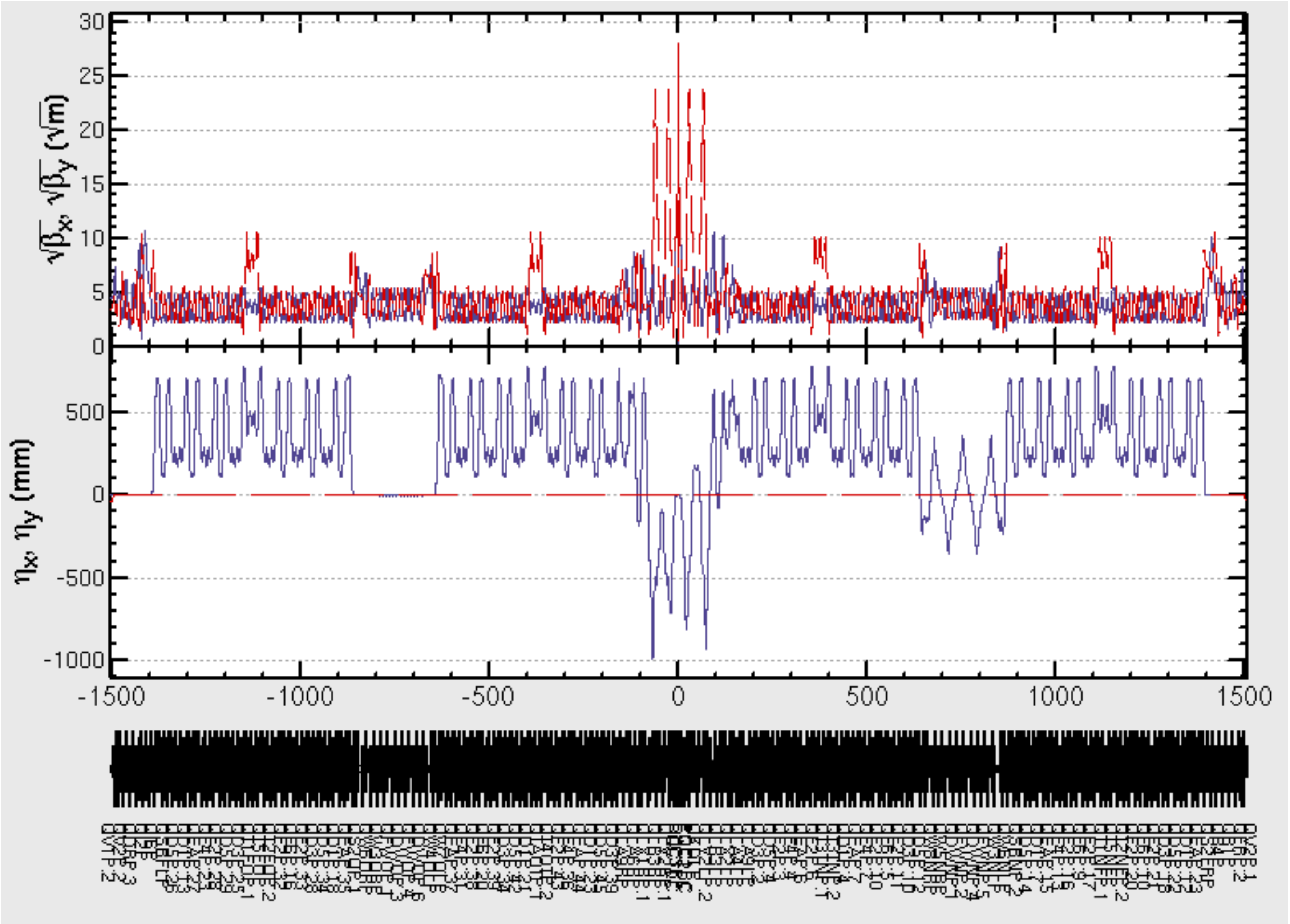

Practical examples

- Hamiltonian and canonical variables used in SAD [1]

The primary position variables are (x, y, s), where x and y are the displacements along the normal and binormal vectors, $\boldsymbol{n}$ and $\boldsymbol{b}$, respectively. Let $\boldsymbol{t}$ denote the tangential vector along s, then $\boldsymbol{n}$, $\boldsymbol{b}$, $\boldsymbol{t}$ consist a right-handed system.
The action in t is expressed by

$$S = \int L_t c dt \ , \tag{2}$$

$$L_t = -\frac{mc}{p_0}\sqrt{1 - \dot{x}^2 + \dot{y}^2 + (1 + x/\rho)^2 \dot{s}^2} + a_x \dot{x} + a_y \dot{y} + (1 + x/\rho) a_s \dot{s} \ , \tag{3}$$

where p_0 and $(a_x, a_y, a_z) = e(A_x, A_y, A_z)/p_0$ are the design momentum and the normalized vector potentials, respectively, and $\dot{}$ denotes the derivative by ct. SAD's coordinate only has the radius of curvature ρ in the local x-s plane. Note that ρ is the curvature of the coordinate system, not that of the orbit. The transverse vector potentials (a_x, a_y) are non-zero only in the solenoid region, where $1/\rho$ is zero.
Currently SAD does not handle the electrostatic potential.
As SAD uses s for the independent variable instead of t, the Lagrangean L for s is written as

$$L = L_t \frac{dct}{ds} \ , \tag{4}$$

$$= -\frac{mc}{p_0}\sqrt{c^2 t'^2 - x'^2 + y'^2 + (1 + x/\rho)^2} + a_x x' + a_y y' + (1 + x/\rho) a_s \ , \tag{5}$$

where $'$ is the derivative by s.

[1] https://acc-physics.kek.jp/SAD/

Practical examples

- Hamiltonian and canonical variables used in SAD [1]

The Lagrangean L defines the *canonical* momenta as

$$p_x = \frac{\partial L}{\partial x'} = \frac{mcx'}{p_0\sqrt{c^2t'^2 - x'^2 - y'^2 - (1 + x/\rho)^2}} + a_x \ , \tag{6}$$

$$p_y = \frac{\partial L}{\partial y'} = \frac{mcy'}{p_0\sqrt{c^2t'^2 - x'^2 - y'^2 - (1 + x/\rho)^2}} + a_y \ , \tag{7}$$

$$p_t = \frac{\partial L}{\partial t'} = -\frac{mc^3t'}{p_0\sqrt{c^2t'^2 - x'^2 - y'^2 - (1 + x/\rho)^2}} \ , \tag{8}$$

which derives the Hamiltonian as

$$H_t = x'p_x + y'p_y + t'p_t - L \tag{9}$$

$$= -\left(\sqrt{-c^2m^2/p_0^2 + p_t^2/c^2 - (p_x - a_x)^2 + (p_y - a_y)^2} + a_s\right)\left(1 + \frac{x}{\rho}\right) \ . \tag{10}$$

[1] https://acc-physics.kek.jp/SAD/

Practical examples

Instead of the canonical variables (t, p_t), SAD uses another set (z, p), The variable z means the logitudinal postion, and p the total momentum, which is more convenient than p_t especially in a low-energy case, ie., $\gamma \sim 1$. The canonical variables (z, p) as well as the Hamiltonian H are obtained using a mother function

$$
\begin{aligned}
G =& G(p_t, z) = \frac{z}{c}\sqrt{p_t^2 - m^2c^4/p_0^2} - t_0(s) \ , && (11) \\
p =& \frac{\partial G}{\partial z} = \frac{\sqrt{p_t^2 p_0^2 - m^2c^4}}{p_0} \ , && (12) \\
t =& \frac{\partial G}{\partial p_t} = -z\frac{\sqrt{p^2 p_0^2 - m^2c^2}}{cpp_0} + t_0(s) \ , && (13) \\
H =& H_t - \frac{\partial G}{\partial s} && (14) \\
=& -\left(\sqrt{p^2 - (p_x - a_x)^2 - (p_y - a_y)^2} + a_s\right)\left(1 + \frac{x}{\rho}\right) + \frac{E}{p_0 v_0} \ , && (15)
\end{aligned}
$$

where $t_0(s)$ is the *design arrival time* at location s, $E = \sqrt{m^2c^4 + p_0^2 p^2}$ the energy of the particle, and $v_0 = 1/t_0'(s)$ the design velocity. The longitudinal position z is written as

$$z = -v\left(t - t_0(s)\right) \ , \tag{16}$$

where v is the total velocity of the particle. Note that $z > 0$ for the head of a bunch.

Thus the canonical variables in SAD are:

$$(x, p_x, y, p_y, z, \delta \equiv p - 1) \ . \tag{17}$$

[1] https://acc-physics.kek.jp/SAD/

Practical examples

- Normal quadrupole

$$\vec{A} \equiv (A_x, A_y, A_s) = (0,0,\frac{1}{2}B_1(y^2 - x^2))$$

$$B_1 = \frac{\partial B_y}{\partial x} \qquad K_1 = \frac{B_1}{B_0\rho}$$

- Solenoid

$$\vec{B} = (0,0,B_s) \qquad \vec{A} \equiv (A_x, A_y, A_s) = (-\frac{1}{2}B_s y, \frac{1}{2}B_s x, 0)$$

- Drift is nonlinear [1]. The exact transfer map $e^{:H:}$ is:

$$H(x,p_x,y,p_y,z,\delta) = \left(-\sqrt{(1+\delta)^2 - p_x^2 - p_y^2} + E/v_0\right)L$$

$$\begin{aligned}
x_2 &= x_1 + \frac{p_{x1}}{\sqrt{p^2 - p_{x1}^2 - p_{y1}^2}}L,\\
p_{x2} &= p_{x1},\\
y_2 &= y_1 + \frac{p_{y1}}{\sqrt{p^2 - p_{x1}^2 - p_{y1}^2}}L,\\
p_{y2} &= p_{y1},\\
z_2 &= z_1 - \left(\frac{p}{\sqrt{p^2 - p_{x1}^2 - p_{y1}^2}} - \frac{v}{v_0}\right)L
\end{aligned}$$

- Leading-order terms of a drift:

$$H(x,p_x,y,p_y,z,\delta) = \left(\frac{p_x^2 + p_y^2}{2(1+\delta)} + \boxed{\frac{(p_x^2 + p_y^2)^2}{8(1+\delta)^3}}\right)L$$

- The drift near the interaction point (IP) contributes to fourth-order geometric nonlinearity (p_y^4 term) and high-order chromaticity (δ-dependence). The p_y^4 term can dominate the nonlinearity of the whole ring when β_y^* is extremely small and L^* is relatively large [1]. This is the case of SuperKEKB and future e+e- circular colliders.

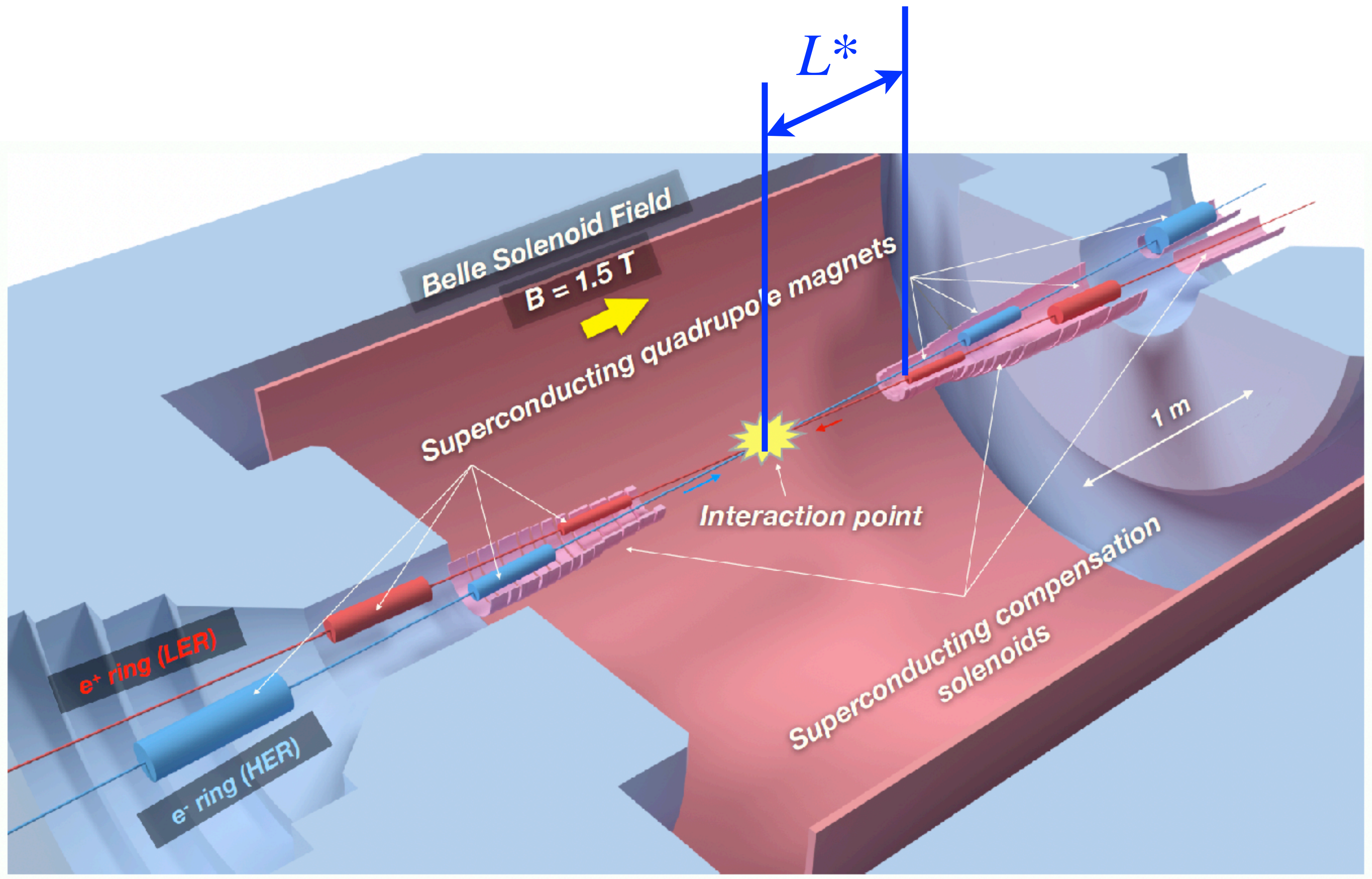

Courtesy of Y. Arimoto

[1] K. Oide and H. Koiso, Phys. Rev. E 47, 2010 (1993).

Practical examples

- The detector solenoid overlaps the drift around the IP:

$$H(x,p_x,y,p_y,z,\delta) = \frac{E}{P_0 v_0} - \sqrt{p^2 - (p_x + \frac{1}{2}b_z y)^2 - (p_y - \frac{1}{2}b_z x)^2}$$

- The transfer map is exact and symplectic:

$$\begin{aligned}
x_2 &= x_1 + \frac{(1+\delta)\sin\phi}{b_z}p_{xi} + \frac{(1+\delta)(1-\cos\phi)}{b_z}p_{yi},\\
y_2 &= y_1 - \frac{(1+\delta)(1-\cos\phi)}{b_z}p_{xi} + \frac{(1+\delta)\sin\phi}{b_z}p_{yi},\\
p_{x2} &= p_{xi}\cos\phi + p_{yi}\sin\phi - \frac{b_z}{2(1+\delta)}y_2,\\
p_{y2} &= -p_{xi}\sin\phi + p_{yi}\cos\phi + \frac{b_z}{2(1+\delta)}x_2,\\
z_2 &= z_1 + \left[\frac{\sqrt{1-p_{xi}^2-p_{yi}^2}-1}{\sqrt{1-p_{xi}^2-p_{yi}^2}} - \Delta v\right]L
\end{aligned}$$

$$\begin{aligned}
\phi &= \frac{b_z L}{(1+\delta)\sqrt{1-p_{xi}^2-p_{yi}^2}},\\
p_{xi} &= p_{x1} + \frac{b_z y_1}{2(1+\delta)},\\
p_{yi} &= p_{y1} - \frac{b_z x_1}{2(1+\delta)},\\
\Delta v &= \frac{v_0 - v}{v_0}
\end{aligned}$$

- The large crossing angle for collision makes the transfer maps around IP extremely complicated. Only approximated maps can be implemented.

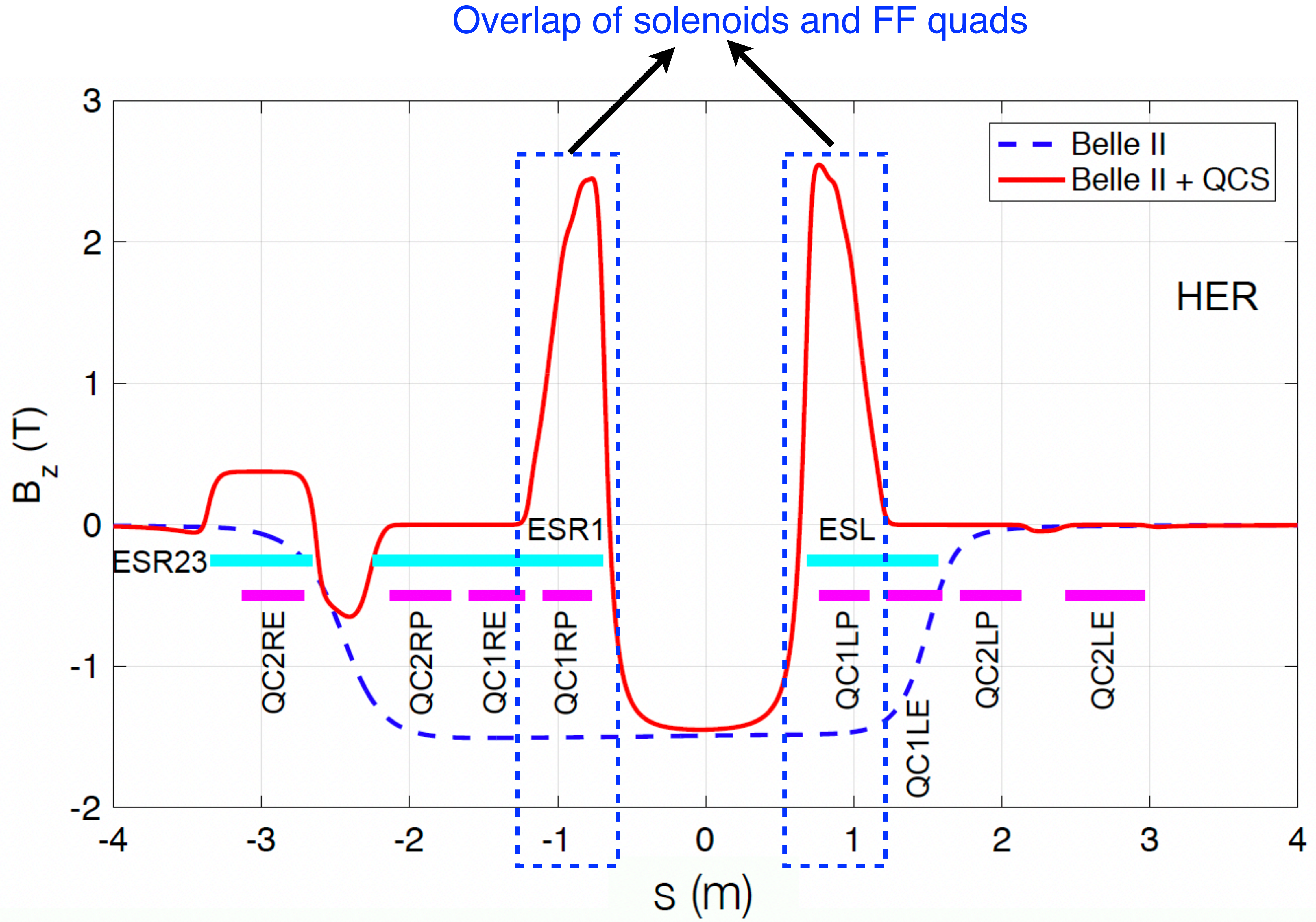

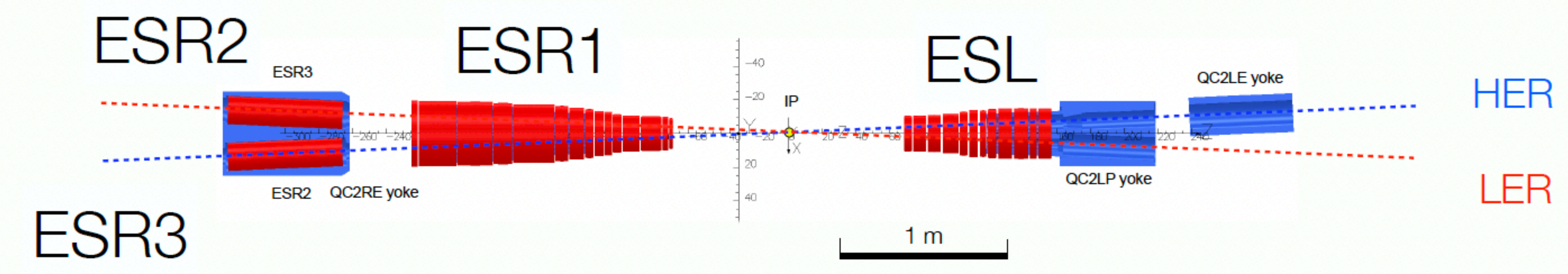

Courtesy of Y. Arimoto

Practical examples

- Special techniques are used to model the interaction region (IR) of SuperKEKB [1].

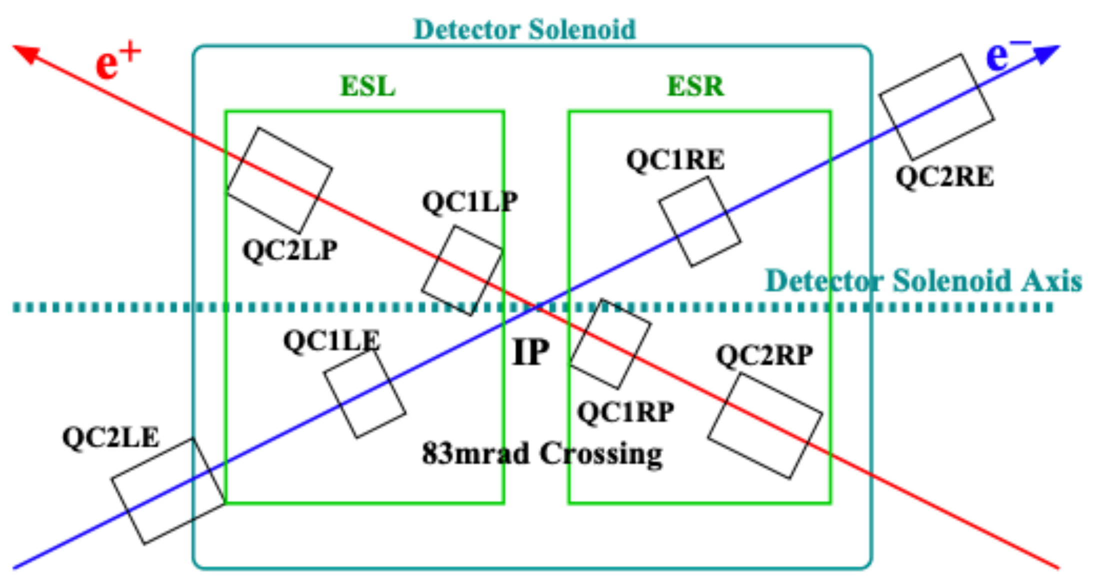

Figure 1: The magnet and orbit layout of the SuperKEKB IR: ESs are the compensation solenoids. QC1s and QC2s are the separated vertical and horizontal focusing superconducting quadrupole magnets, respectively.

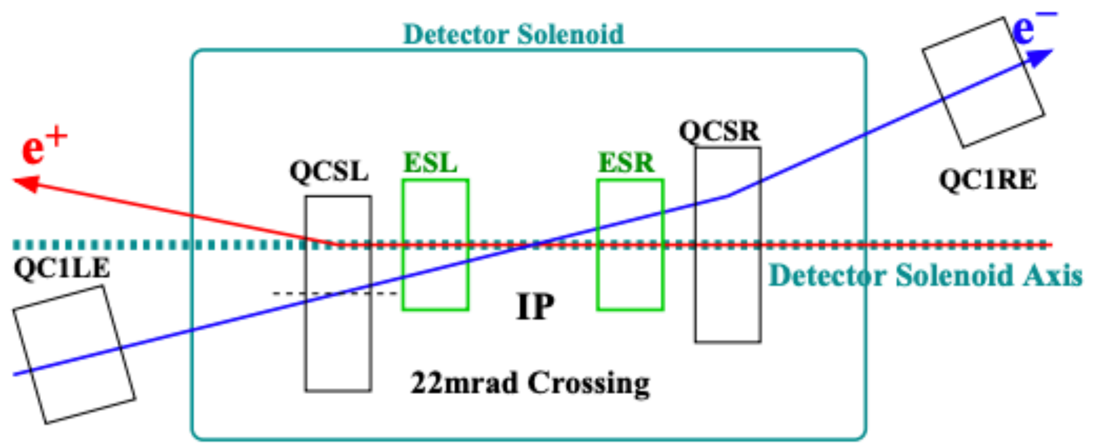

Figure 2: The magnet and orbit layout of the KEKB IR: ESs are the compensation solenoids. QCSs are the shared vertical focusing superconducting quadrupole magnets. QC1s are the additional vertical focusing normal-conducting quadrupole magnets for the electron beam.

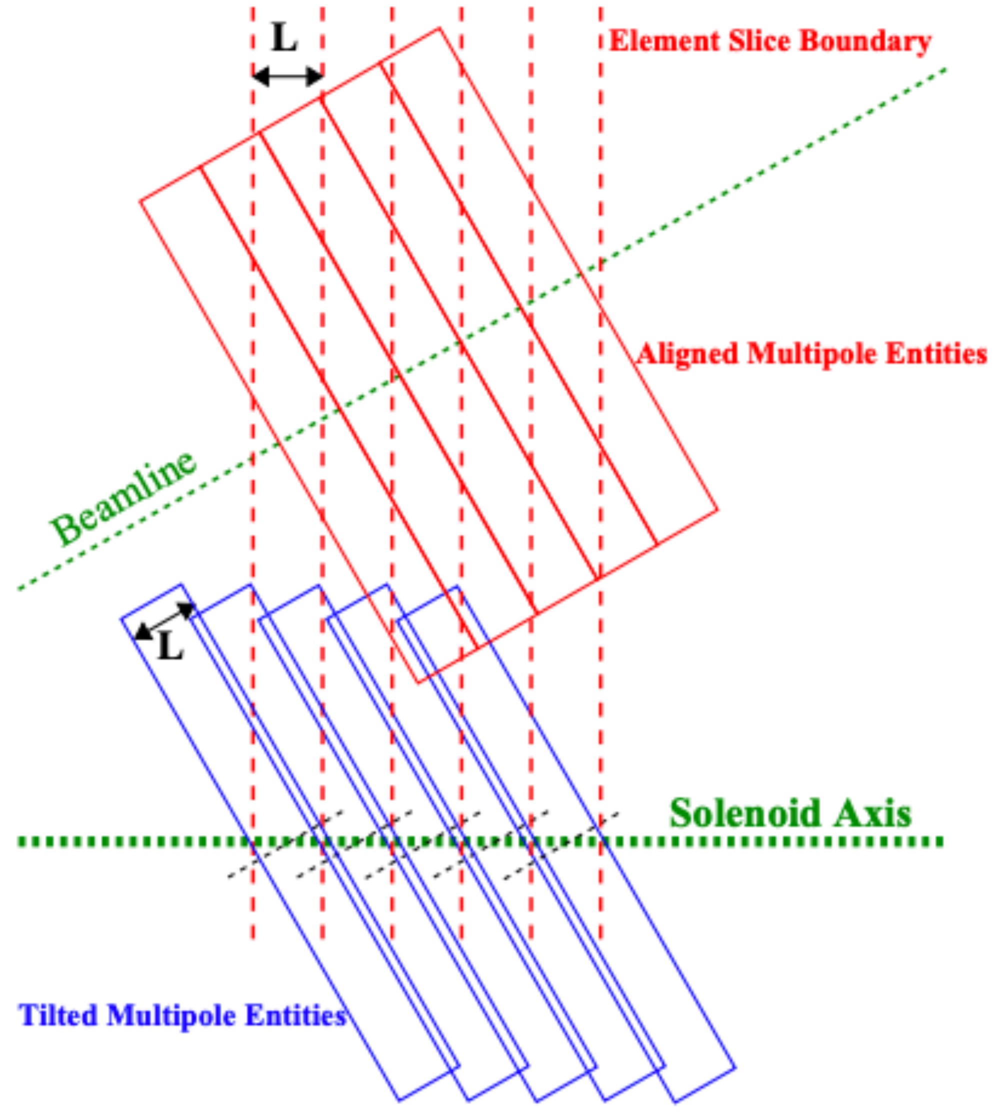

Figure 3: The multipole element boundary and the multipole field location in the lattice modeling: The red dashed-lines show the boundary of the multipole element slice aligned on the solenoid axis. The blue solid boxes show the titled multipole field entities in the element slice. The red solid boxes show the multipole field entities aligned on the beamline.

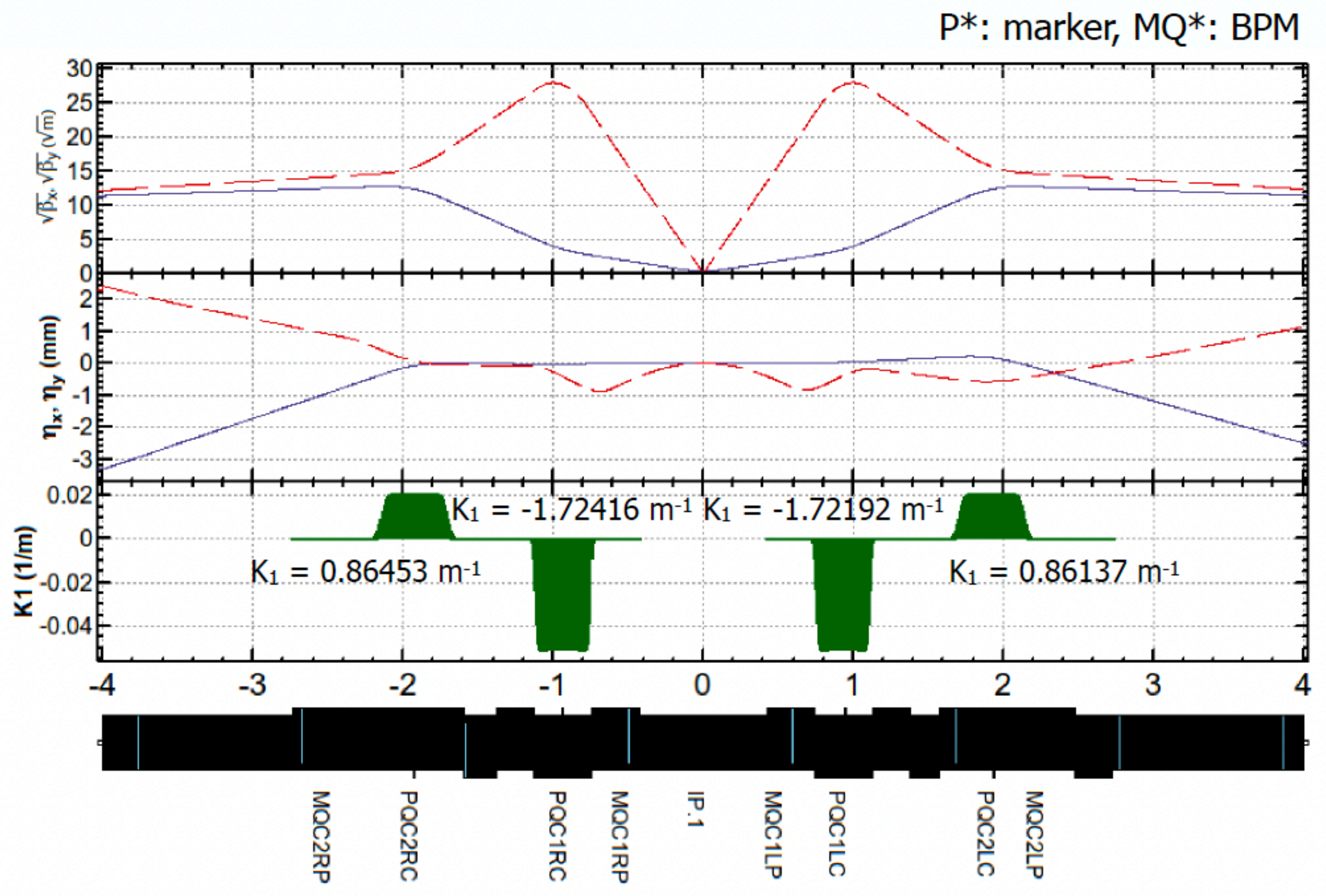

QC2RP	QC1RP	QC1LP	QC2LP
$\Delta\theta = -0.121^\circ$	$\Delta\theta = +0.413^\circ$	$\Delta\theta = -0.782^\circ$	$\Delta\theta = -0.213^\circ$
$\Delta y = -1.0\ mm$	$\Delta y = -1.0\ mm$	$\Delta y = -1.5\ mm$	$\Delta y = -1.5\ mm$

QC1 and QC2 BPMs: same offset of the magnet coil

[1] A. Morita et al., "SuperKEKB interaction region modeling".

Practical examples

- Dipole soft fringe map (implemented in SAD and imported to Bmad [1])

Bmad defines the bend soft edge map in terms of the field integral F_{H1} for the entrance end and F_{H2} for the exit end given by (see Eq. (3.5))

$$F_{H1} \equiv F_{int}\, H_{gap} = \int_{pole} ds\, \frac{B_y(s)\,(B_{y0} - B_y(s))}{2\,B_{y0}^2} \tag{19.46}$$

With a similar equation for F_{H2}. The soft edge map is then

$$\begin{aligned} x_2 &= x_1 + c_1\, p_z \\ p_{y2} &= p_{y1} + c_2\, y_1 - c_3\, y_1^3 \\ z_2 &= z_1 + \frac{1}{1+p_{z1}} \left(c_1\, p_{x1} + \frac{1}{2}\, c_2\, y_1^2 - \frac{1}{4}\, c_3\, y_1^4 \right) \end{aligned} \tag{19.47}$$

For the entrance face:

$$c_1 = \frac{g_{tot}\, F_{H1}^2}{2\,(1+p_z)}, \qquad c_2 = \frac{2\, g_{tot}^2\, F_{H1}}{1+p_z}, \qquad c_3 = 0 \tag{19.48}$$

with `g_tot` is the total bending strength

$$g_{tot} = \mathrm{g} + \mathrm{g\_err} \tag{19.49}$$

`g` being the reference bend strength and `g_err` being bend the difference between the actual and reference bend strengths (§3.5).

For the exit face, the subsitution is made

$$\begin{aligned} F_{H1} &\to F_{H2} \\ g_{tot} &\to -g_{tot} \end{aligned} \tag{19.50}$$

When the SAD bend soft edge map is used (§4.20), the map is the same except that the value of c_3 is

$$c_3 = \frac{8\, g_{tot}^2}{F_{H1}\,(1+p_z)} \tag{19.51}$$

- Quadrupole soft fringe map (implemented in SAD and imported to Bmad [1])

Only the quadrupole soft edge fringe is modeled in *Bmad*. The model is adapted from SAD[SAD]. The fringe map is:

$$\begin{aligned} x_2 &= x_1\, e^{g_1} + g_2\, p_{x1} \\ p_{x2} &= p_{x1} e^{-g_1} \\ y_2 &= y_1\, e^{-g_1} - g_2\, p_{y1} \\ p_{y2} &= p_{y1} e^{g_1} \\ z_2 &= z_1 - \left[g_1\, x_1\, p_{x1} + g_2 \left(1 + \frac{g_1}{2}\right) e^{-g_1}\, p_{x1}^2 \right] + \left[g_1\, y_1\, p_{y1} + g_2 \left(1 - \frac{g_1}{2}\right) e^{g_1}\, p_{y1}^2 \right] \end{aligned} \tag{19.53}$$

where

$$\begin{aligned} g_1 &= K_1\, \mathrm{fq1} \\ g_2 &= K_1\, \mathrm{fq2} \end{aligned} \tag{19.54}$$

K_1 is the quadrupole strength, and `fq1` and `fq2` are the fringe quadrupole parameters. These parameters are related to the field integral I_n via

$$\begin{aligned} \mathrm{fq1} &= I_1 - \frac{1}{2}\, I_0^2 \\ \mathrm{fq2} &= I_2 - \frac{1}{3}\, I_0^3 \end{aligned} \tag{19.55}$$

where I_n is defined by

$$I_n = \frac{1}{K_1} \int_{-\infty}^{\infty} \left(K_1(s) - H(s-s_0)\, K_1\right) (s-s_0)^n\, ds \tag{19.56}$$

and $H(s)$ is the step function

$$H(s) = \begin{cases} 1 & s > 0 \\ 0 & s < 0 \end{cases} \tag{19.57}$$

and it is assumed that the quadrupole edge is at s_0 and the interior is in the region $s > s_0$.

[1] Bmad manual

Practical examples

- Maxwellian hard-edge fringe maps are important sources of nonlinearity in storage rings.
- General equations were developed (E. Forest et al.) and apply for BEND, QUAD, SEXT, …

The magnetic multipole hard edge fringe field is modeled using the method shown in Forest[Forest98]. For the m^{th} order multipole the Lee transform is (Forest Eq. (13.29):

$$
\begin{aligned}
f_\pm &= \mp\Re\left[\frac{(b_m + i\,a_m)\,(x+i\,y)^{m+1}}{4\,(m+2)\,(1+\delta)}\left\{x\,p_x + y\,p_y + i\frac{m+3}{m+1}(x\,p_x - y\,p_y)\right\}\right] \\
&\equiv \frac{p_x\,f^x + p_y\,f^y}{1+\delta}
\end{aligned}
\tag{19.58}
$$

The multipole strengths a_m and b_m are given by (14.9) and the second equation defines f^x and f^y. On the right had side of the first equation, the minus sign is appropriate for particles entering the magnet and the plus sign is for particle leaving the magnet. Notice that here the multipole order m is equivalent to $n-1$ in Forest's notation.

With this, the implicit multipole map is (Forest Eq. (13.31))

$$
\begin{aligned}
x^f &= x - \frac{f^x}{1+\delta} \\
p_x &= p_x^f - \frac{p_x^f\,\partial_x f^x + p_y^f\,\partial_x f^y}{1+\delta} \\
y^f &= y - \frac{f_y}{1+\delta} \\
p_y &= p_y^f - \frac{p_x^f\,\partial_y f^x + p_y^f\,\partial_y f^y}{1+\delta} \\
\delta^f &= \delta \\
z^f &= \frac{p_x^f\,f^x + p_y^f\,f^y}{(1+\delta)^2}
\end{aligned}
\tag{19.59}
$$

- Maxwellian hard-edge fringe map of a BEND is particular. Its pole profile can be round or flat.

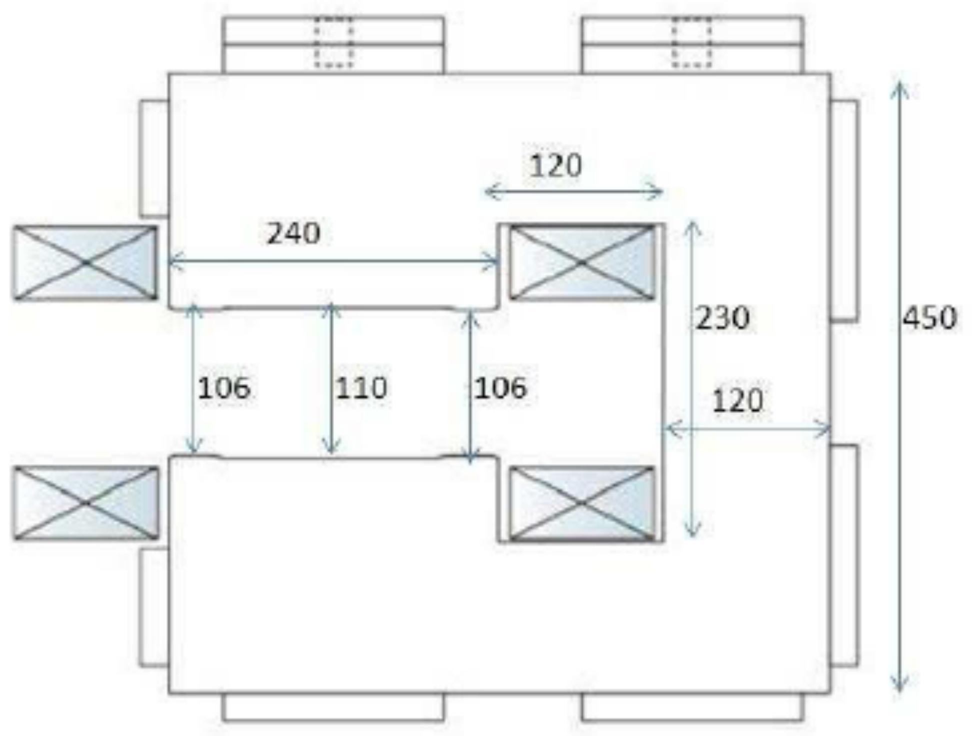

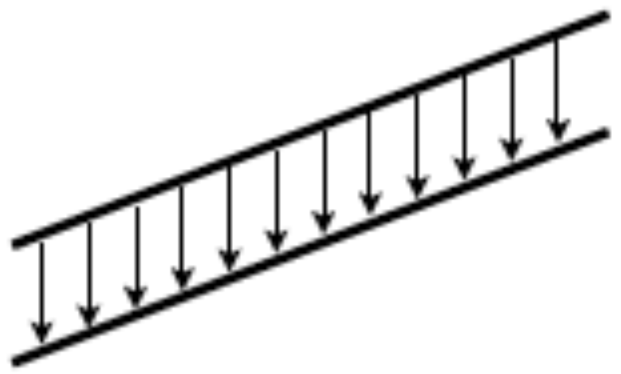

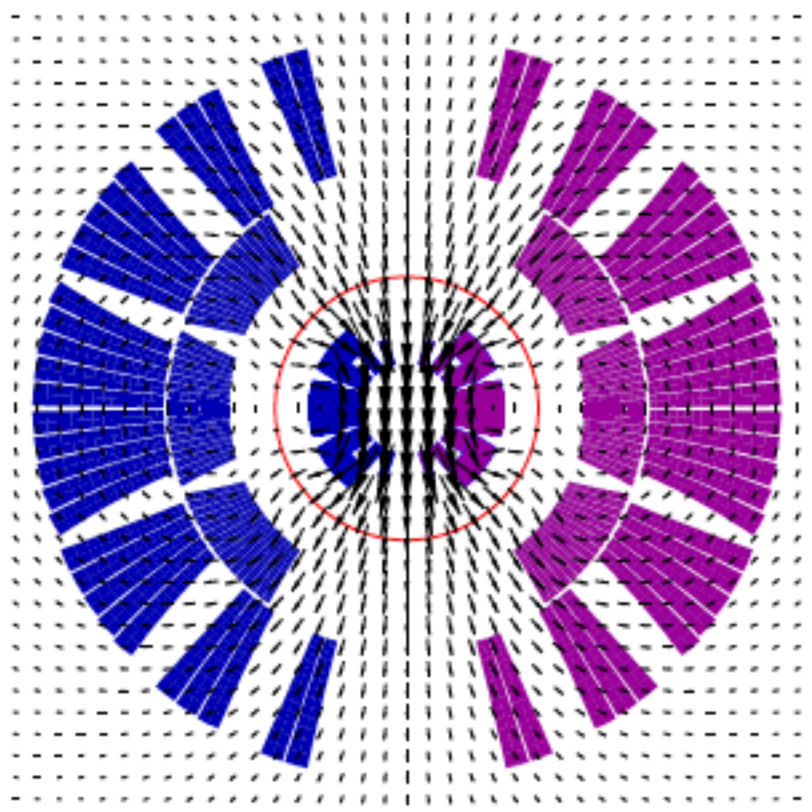

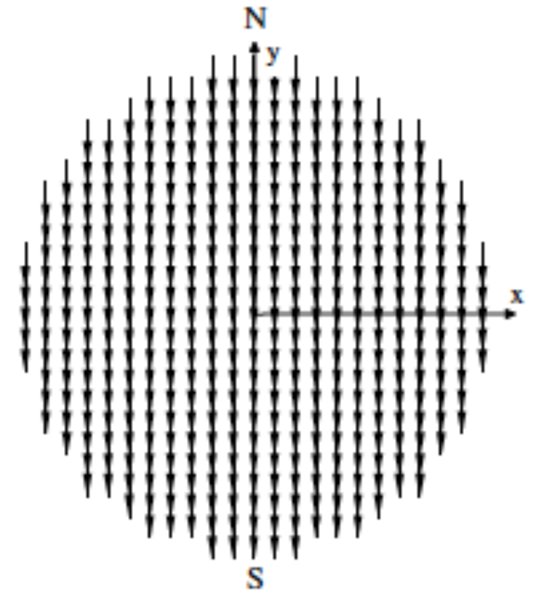

[1] Bmad manual

Practical examples

- IP drift and Maxwellian hard-edge fringe fields of final focus (FF) quads are the dominant sources of nonlinearity in SuperKEKB and future e+e- circular colliders.
- The scaling law was found by Oide and Koiso [1]. The SuperKEKB case was investigated by Ohmi and Koiso [2]. A simple scaling law describes the “level of challenge”:

$$J_y \leq \frac{\beta_y^{*2}}{(1+2|K|L^{*2}/3)L^*} A(\mu_y)$$

Ring	β_y^* [μm]	K=k_1 [m^{-2}]	L* [m]	J_y/A [μm]
SuperKEKB HER	300	-3.1	1.22	0.018
SuperKEKB LER	270	-5.1	0.76	0.032
CEPC	1200	-0.176	1.5	0.76
TLEP(BINP design)	1000	-0.16	0.7	1.36
KEKB	5900	-1.779	1.762	4.22

~ 1/20

< 1/100

Courtesy of Y. Ohnishi

- The scaling law concluded that SuperKEKB is 100 times more challenging than KEKB.
- CEPC (and STCF?) is less challenging than SuperKEKB.

[1] K. Oide and H. Koiso, Phys. Rev. E 47, 2010 (1993). [2] K. Ohmi and H. Koiso, TUPEB015, IPAC’10

Practical examples

- "Feed-down" effect

- Feed-down: The magnetic multipoles are usually parametrized through the formula

$$B_y + iB_x = B_0 \sum_{n=0}^{\infty} (b_n + ia_n)(x+iy)^n, \tag{4.1}$$

where B_0 is the design bending field and b_n, a_n are the normal and skew multipole strengths with the dimension m^{-n}. Given Eq.(4.1) for the magnetic field, it follows that the potential function V is given by

$$V = \theta_d \mathrm{Re} \sum_{n=0}^{\infty} \frac{1}{n+1}(b_n + ia_n)(x+iy)^{n+1}. \tag{4.2}$$

The feed-down is calculated by generalizing Eq.(4.2) to

$$V = \theta_d \mathrm{Re} \sum_{n=0}^{\infty} \frac{1}{n+1}(b_n + ia_n)[x + \Delta x + i(y+\Delta y)]^{n+1}, \tag{4.3}$$

where Δx and Δy is the horizontal and vertical orbit. If we restrict ourselves to terms linear in Δx or Δy, we find the following contributions from the feed-down

$$a_{n-1} = n(a_n \Delta x + b_n \Delta y) + O(2), \tag{4.4}$$

$$b_{n-1} = -n(a_n \Delta y - b_n \Delta x) + O(2). \tag{4.5}$$

The general formulation of feed-down is to respectively replace x and y by $x+\Delta x$ and $y+\Delta y$ in Eq.(4.1) and expand it into series [10]. Then the feed-down harmonics due to (a_n, b_n) harmonics can be calculated. The relevant monomials associated with a given order k are

$$b_k + ia_k = (b_n + ia_n)\left[\frac{n!}{k!(n-k)!}\right](\Delta x + i\Delta y)^{n-k}. \tag{4.6}$$

For example, with $k = n-1$ the above equation gives Eqs.(4.4) and (4.5). Here American convention is used, $n = 0$ indicates a dipole field, $n = 1$ indicates a quadrupole field, etc.

In principle, with non-zero orbit offset, the $n-$order harmonics can generate harmonics of all orders from 0 (dipole) to $n-1$ (multipole). Especially, feed-down is important in the interaction region (IR) of SuperKEKB where the closed orbit is offsetted from the magnetic center, and the quadrupole magnets are offsetted to compensate the dipole field of detector solenoids and anti-solenoids.

- Chromatic perturbations: The chromatic perturbations can be treated as a feed-down where the orbit is given by the nonlinear dispersion function η

$$\Delta x = \delta\eta = \delta(\eta_0 + \delta\eta_1 + ...), \tag{4.7}$$

where η_0 is the linear dispersion function. Furthermore, the multipole strength is replaced by an effective multipole strength given by

$$b_n = \frac{1}{1+\delta} b_n. \tag{4.8}$$

Practical examples

- For SuperKEKB, the 4th-order quad fringe map was downgraded to 3rd-order nonlinearity due to magnet offsets and closed orbit. A $p_x^2 p_y$ term was identified to cause a significant luminosity loss in simulations.

```
In[1]:= (*f1=K1/(12(1+δ)L)*)
HQfr = f1*((x^3 + 3 x*y^2) px - (y^3 + 3 x^2 y) py);
D[HQfr, x]*ΔX
D[HQfr, px]*ΔPX
D[HQfr, y]*ΔY
D[HQfr, py]*ΔPY
Out[2]= f1 (-6 py x y + px (3 x^2 + 3 y^2)) ΔX
Out[3]= f1 (x^3 + 3 x y^2) ΔPX
Out[4]= f1 (6 px x y - py (3 x^2 + 3 y^2)) ΔY
Out[5]= f1 (-3 x^2 y - y^3) ΔPY
```

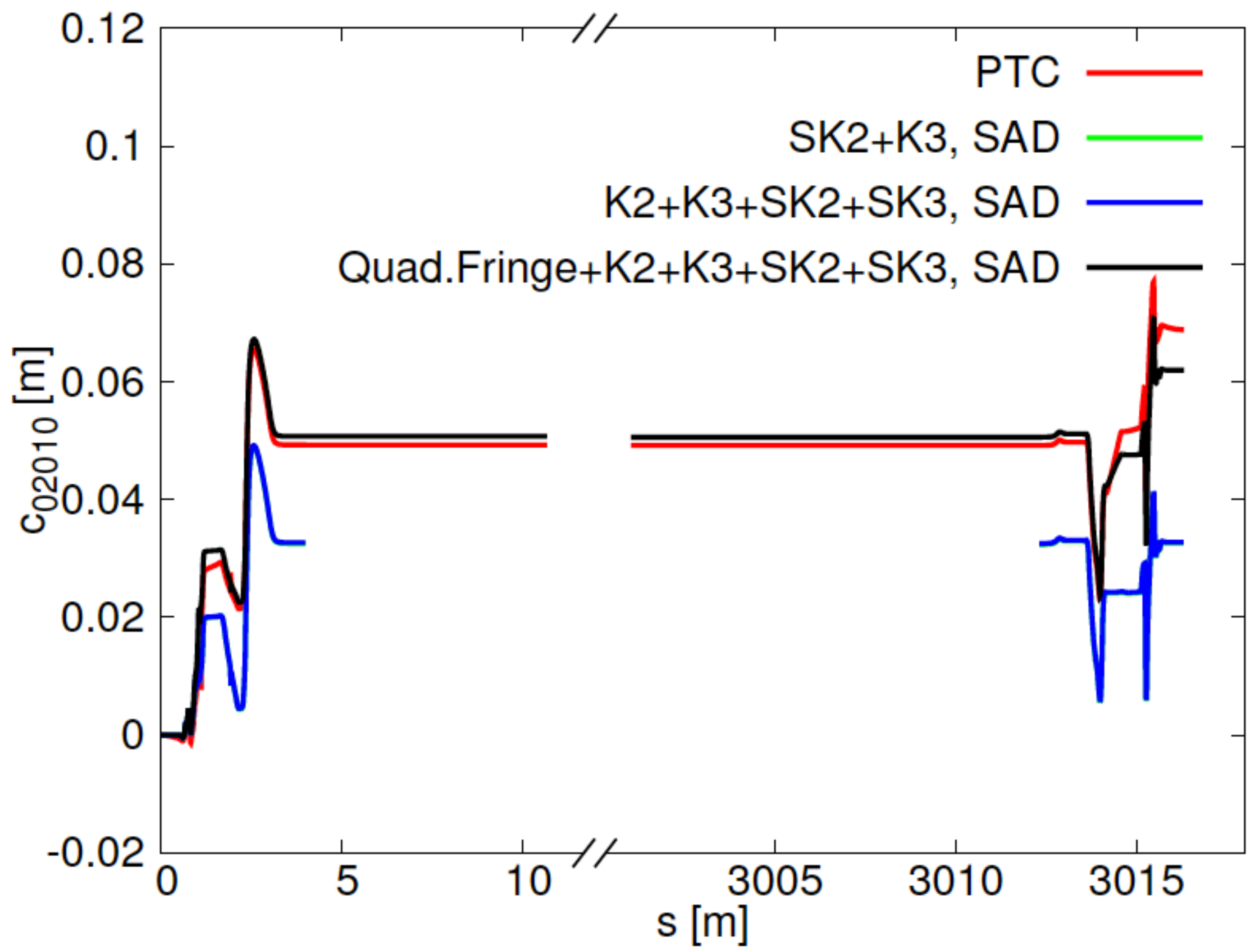

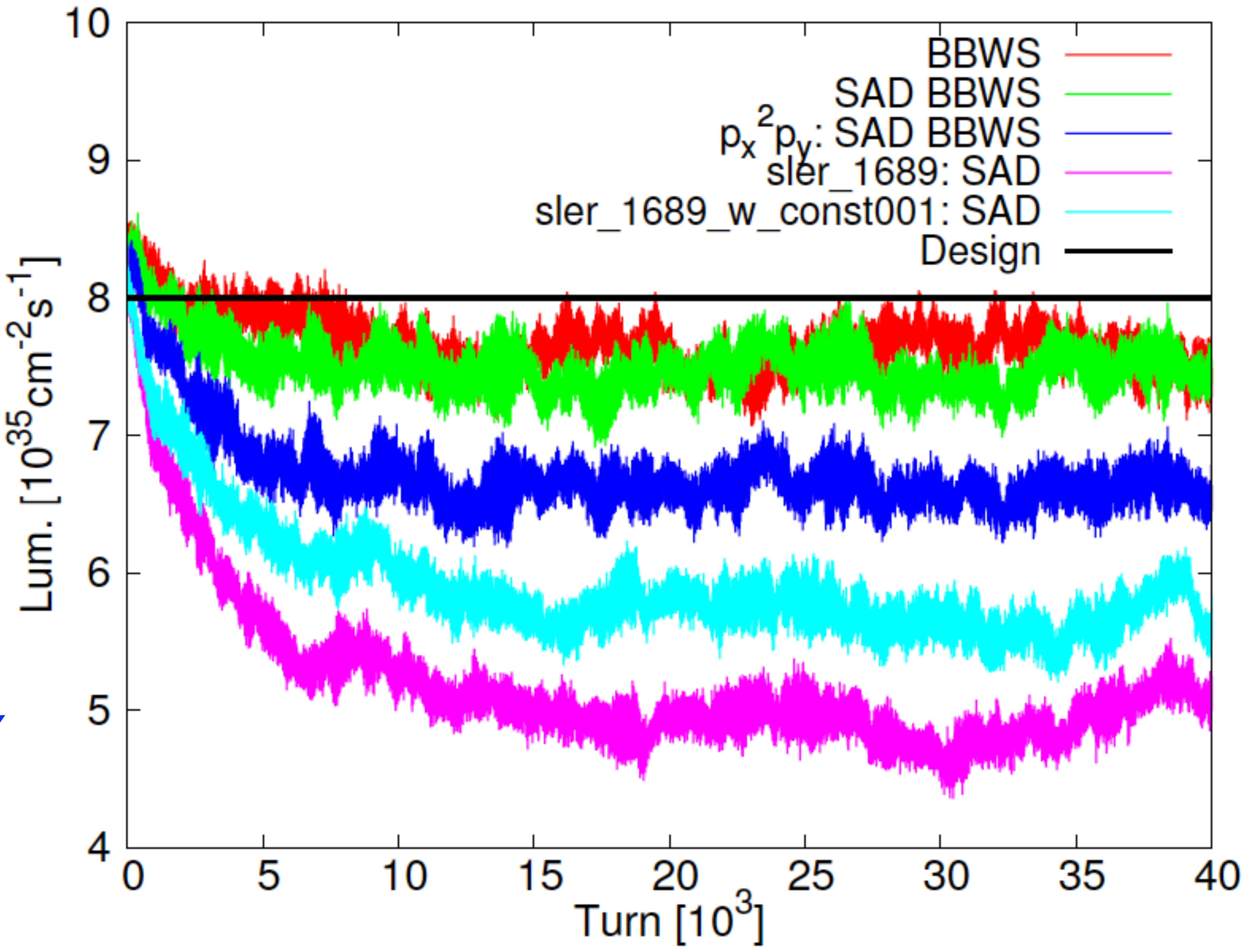

From transfer maps to nonlinear analysis

- Lie formulations: Dragt-Forest paper (1983)

Computation of nonlinear behavior of Hamiltonian systems using Lie algebraic methods [a)]

Alex J. Dragt[b)] and Etienne Forest[b),c)]
Center for Theoretical Physics, Department of Physics and Astronomy, University of Maryland, College Park, Maryland 20742

(Received 15 March 1983; accepted for publication 18 July 1983)

Lie algebraic methods are developed to describe the behavior of trajectories near a given trajectory for general Hamiltonian systems. A procedure is presented for the computation of nonlinear effects of arbitrarily high degree, and explicit formulas are given through effects of degree 5. Expected applications include accelerator design, charged particle beam and light optics, other problems in the general area of nonlinear dynamics, and, perhaps, with suitable modification, the area of S-matrix expansions in quantum field theory.

8. COMPUTATION OF H_R^{int}

By definition, H_R consists of terms of degree 3 and higher,

$$H_R = H_3 + H_4 + \cdots . \tag{8.1}$$

Also, in view of (6.10) and the fact that $\mathcal{M}_2$ produces a linear transformation when acting on ζ^{in} [see (7.7)], it follows that H_R^{int} has the decomposition

$$H_R^{\text{int}} = H_3^{\text{int}} + H_4^{\text{int}} + \cdots , \tag{8.2}$$

where each term H_m^{int} is a homogeneous polynomial of degree m given by the relation

$$H_m^{\text{int}}(\zeta^{\text{in}}, t) = H_m(\mathcal{M}_2\, \zeta^{\text{in}}, t). \tag{8.3}$$

To see how this works out in a specific case, consider the computation of H_3^{int}. The terms of still higher degree are handled analogously. Suppose that H_3 is written in the explicit form

$$H_3(\zeta^{\text{in}}, t) = \sum_{abc} T_{abc}(t)\, \zeta_a^{\text{in}} \zeta_b^{\text{in}} \zeta_c^{\text{in}}, \tag{8.4}$$

where T_{abc} is a set of (possibly time-dependent) coefficients. Then use of (8.3) gives the relation

$$H_3^{\text{int}}(\zeta^{\text{in}}, t) = \sum_{abc} T_{abc}(\mathcal{M}_2\, \zeta_a^{\text{in}})(\mathcal{M}_2\, \zeta_b^{\text{in}})(\mathcal{M}_2\, \zeta_c^{\text{in}}). \tag{8.5}$$

From transfer maps to nonlinear analysis

- Lie formulations: Irwin-Wang paper (1996)

EXPLICIT SOFT FRINGE MAPS OF A QUADRUPOLE

John Irwin and Chun-xi Wang
Stanford Linear Accelerator Center, Stanford University, Stanford, CA 94309 USA

III. NON-LINEAR FRINGE MAP

Consider the map from the center of the quadrupole $s_1 = 0$ to a point s_2 that is far outside the fringe field region. Our goal is to find a simplectic fringe map $\mathcal{Q}_f$ which represents the fringe field effects so that the map $\mathcal{M}(s_1 \to s_2)$ can be written as

$$\mathcal{M}(s_1 \to s_2) = \mathcal{M}_Q(s_1 \to s_0)\ \mathcal{Q}_f\ \mathcal{M}_{drift}(s_0 \to s_2) \tag{11}$$

where $\mathcal{M}_Q$ is the map of an ideal quadrupole of strength k_0 and length $s_0 = L_{eff}$; $\mathcal{M}_{drift}$ is the drift map from s_0 to s_2. (They may contain kinematic nonlinearity even though we neglect it in our calculation of $\mathcal{Q}_f$. This approximation may not be good at the 6-th order)

Before working on Eq.(11), we concentrate on the non-linear part, i.e. considering

$$\mathcal{M}(s_1 \to s_2) = \mathcal{R}_-(s_1 \to s_0)\ \tilde{\mathcal{Q}}_f\ \mathcal{R}_+(s_0 \to s_2) \tag{12}$$

where $\mathcal{R}_\pm$ are exact linear maps. To calculate this, we choose the perturbation $\tilde{H}(s)$ as in Eq.(5), slice the time dependent Hamiltonians into pieces and move all the linear map before and after s_0 to the left and right side respectively using similarity transformation. This process is exact. Then we concatenate all the nonlinear pieces into a perturbation map $\tilde{\mathcal{Q}}_f$ via 2nd order BCH formula. Since we are concerned with up to 6-th order generators, 3rd and higher order BCH terms do not contribute in this case. Therefore

$$\tilde{\mathcal{Q}}_f = e^{:-\int_{s_1}^{s_2} ds\, \bar{H}(s) + \frac{1}{2}\int_{s_1}^{s_2} ds \int_{s}^{s_2} d\tilde{s}[\bar{H}(s), \bar{H}(\tilde{s})]:} \tag{13}$$

where $\underline{\bar{H}(s) = \tilde{H}(s, R(s_0 \to s)X)}$; X represents the phase space variables and $R(a \to b)$ is the exact linear matrix from a to b.

From transfer maps to nonlinear analysis

- Resonance driving terms (RDTs)

The effective Hamiltonian of a ring can be normalized in resonance bases [Ref. E. Forest, *Beam Dynamics – A New Attitude and Framework*, 1998].

For a ring with n elements, one can normalize the one turn map $\mathcal{M}_{1\to n}$ as [Ref. L. Yang *et al.*, Phys. Rev. ST Accel. Beams 14, 054001 (2011)]

$$\mathcal{M}_{1\to n} = \mathcal{A}_1^{-1} e^{:h:} \mathcal{R}_{1\to n} \mathcal{A}_1,$$

with $\mathcal{R}$: rotation, $e^{:h:}$: nonlinear Lie map, $\mathcal{A}_1$: normalizing map. Assume no coupling (the theory can be generalized for nonzero coupling), $\mathcal{A}_i$ in x plane at the ith element can be approximated in perturbation theory as

$$\mathcal{A}_i x = \sqrt{\beta_{x,i}}x + \eta_{x,i}\delta,$$

$$\mathcal{A}_i p_x = \frac{-\alpha_{x,i}x + p_x}{\sqrt{\beta_{x,i}}} + \eta'_{x,i}\delta.$$

In the resonance basis, using action-angle variables (J, ϕ) one can write

$$h_x^{\pm} \equiv \sqrt{J_x} e^{\pm i\phi_x} = \frac{X \mp iP_x}{\sqrt{2}},$$

$$\mathcal{R}_{i\to j} h_x^{\pm} = \mathcal{R}_{i\to j}\sqrt{J_x} e^{\pm i\phi_x} = e^{\pm i\mu_{i\to j,x}} h_x^{\pm},$$

where $\mu_{i\to j,x}$ is the phase advance of $i \to j$. Consequently, the potential of a multipole magnetic field can be expanded in the resonance bases of h_{abcde} as

$$h = \sum h_{abcde} h_x^{+a} h_x^{-b} h_y^{+c} h_y^{-d} \delta^e.$$

Each h_{abcde} (a complex number in general) drives a certain resonance, and is an explicit function of magnet strengths, beta functions and dispersions.

From transfer maps to nonlinear analysis

- Resonance driving terms (RDTs)

The effective Hamiltonian corresponding to chromaticity is

$$h_c = \sum h_{1100e} h_x^{+1} h_x^{-1} \delta^e + \sum h_{0011e} h_y^{+1} h_y^{-1} \delta^e,$$

$$h_c = J_x \sum h_{1100e} \delta^e + J_y \sum h_{0011e} \delta^e.$$

Then the tunes are calculated as

$$\nu_x = -\frac{1}{2\pi} \frac{\partial h_c}{\partial J_x} = -\frac{1}{2\pi} \sum h_{1100e} \delta^e,$$

$$\nu_y = -\frac{1}{2\pi} \frac{\partial h_c}{\partial J_y} = -\frac{1}{2\pi} \sum h_{0011e} \delta^e.$$

Therefore the RDTs of h_{1100e} and h_{0011e} correspond to linear and high-order chromaticity.

h_{abcde}	Driving effects
h_{11001}, h_{00111}	Linear chromaticity ζ_x, ζ_y
$h_{21000}, h_{12000} \| h_{10110}, h_{01110}$	ν_x $[(J_x)^{3/2}] \| [(J_x)^{1/2}(J_y)]$
$h_{30000}, h_{03000} \| h_{00300}, h_{00030}$	$3\nu_x$ $[(J_x)^{3/2}] \| 3\nu_y$ $[(J_y)^{3/2}]$
$h_{10020}, h_{01200} \| h_{10200}, h_{01020}$	$\nu_x - 2\nu_y \| \nu_x + 2\nu_y$ $[(J_x)^{1/2}(J_y)]$
$h_{20010}, h_{02100} \| h_{20100}, h_{02010}$	$2\nu_x - \nu_y \| 2\nu_x + \nu_y$ $[(J_x)(J_y)^{1/2}]$
$h_{00210}, h_{00120} \| h_{11100}, h_{11010}$	ν_y $[(J_y)^{3/2}] \| [(J_x)(J_y)^{1/2}]$
$h_{22000}, h_{00220}, h_{11110}$	$d\nu_x/dJ_x, d\nu_y/dJ_y, d\nu_{x,y}/dJ_{y,x}$
$h_{40000}, h_{04000} \| h_{00400}, h_{00040}$	$4\nu_x$ $[(J_x)^2] \| 4\nu_y$ $[(J_y)^2]$
$h_{31000}, h_{13000} \| h_{20110}, h_{02110}$	$2\nu_x$ $[(J_x)^2] \| [(J_x)(J_y)]$
$h_{00310}, h_{00130} \| h_{11200}, h_{11020}$	$2\nu_y$ $[(J_y)^2] \| [(J_x)(J_y)]$
$h_{20020}, h_{02200} \| h_{20200}, h_{02020}$	$2\nu_x - 2\nu_y \| 2\nu_x + 2\nu_y$ $[(J_x)(J_y)]$
$h_{30010}, h_{03100} \| h_{30100}, h_{03010}$	$3\nu_x - \nu_y \| 3\nu_x + \nu_y$ $[(J_x)^{3/2}(J_y)^{1/2}]$
$h_{10030}, h_{01300} \| h_{10300}, h_{01030}$	$\nu_x - 3\nu_y \| \nu_x + 3\nu_y$ $[(J_x)^{1/2}(J_y)^{3/2}]$

Table : Low-order driving terms.

Single-particle nonlinear dynamics

- For a storage ring, the particles take periodic motion because of periodic lattice. The nonlinear analysis of transfer maps usually results in strong correlation of dynamics with betatron resonances (X-Y coupling) and synchro-betatron resonances (X-Y-Z coupling):

$$m_x\nu_x + m_y\nu_y = \textbf{Integer}$$

$$m_x\nu_x + m_y\nu_y + m_s\nu_s = \textbf{Integer}$$

- When a storage ring is operating on a resonance, the kicks felt by particles will accumulate from turn to turn, leading to a large amplitude of betatron motion.
- Resonances are generally harmful to the beam quality (characterized by emittances, beam sizes, lifetime, detector background, etc.).
- Taking the fact of $\epsilon_y \ll \epsilon_x \ll \epsilon_z$ (~$1 : 10^3 : 10^6$) at SuperKEKB, any coupling from X- and/or Z-directions would make a significant change to ϵ_y, and consequently reduce luminosity.

- Usually higher-order resonances (= larger number of $|m_x| + |m_y| + |m_s|$) are less harmful than lower-order resonances. The working point $(\nu_{x0}, \nu_{y0}, \nu_{s0})$ should be away from dangerous resonances.
- Sometimes the resonances are correlated with single-particle dynamics, but more often they are correlated with collective effects. Collective effects depend on bunch/beam current.

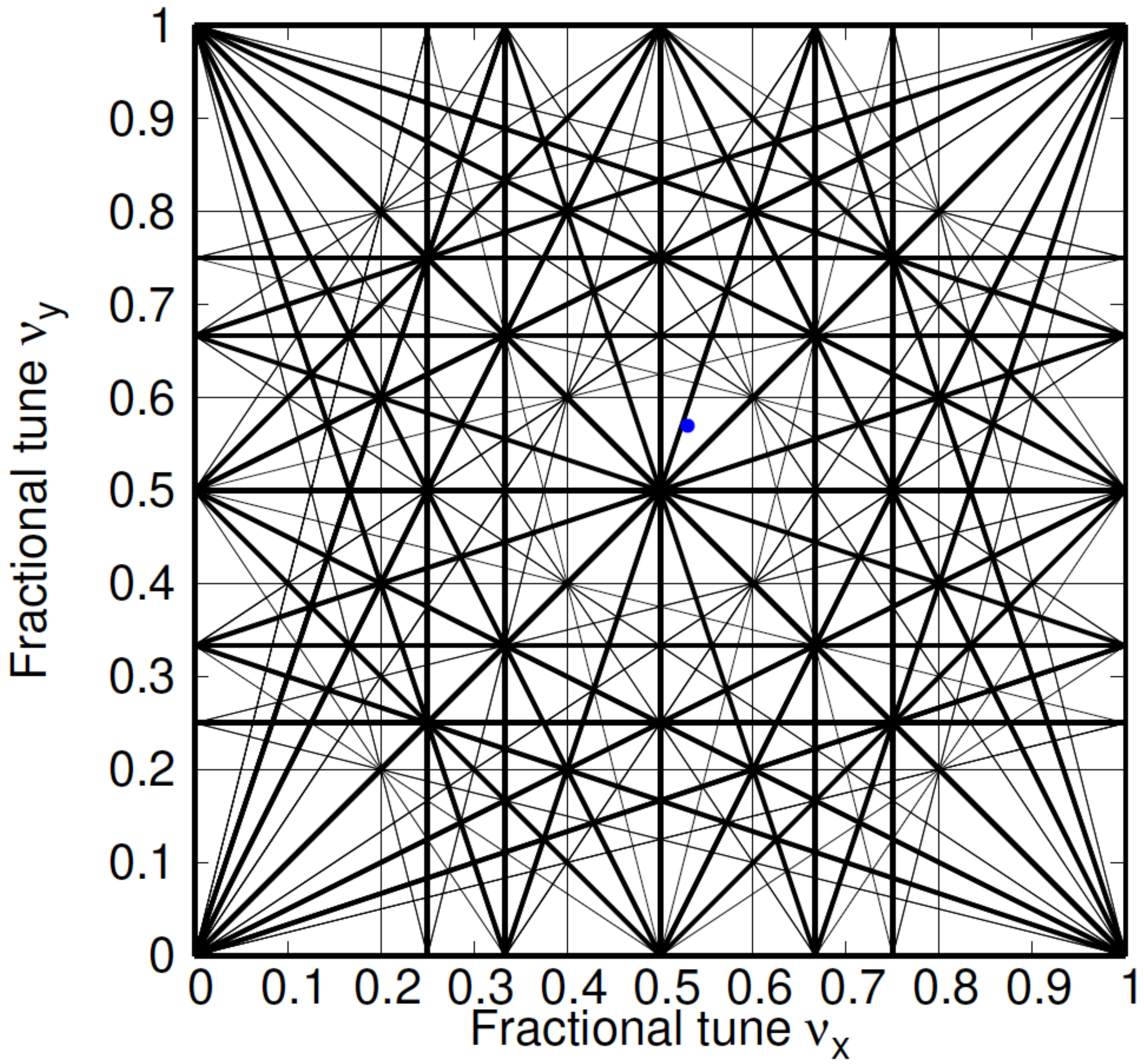

Resonance diagram with $|m_x| + |m_y| \leq 5$. The blue dot shows the design working point of SuperKEKB.

Single-particle nonlinear dynamics

- At SuperKEKB, a list of dangerous resonances can be tentatively given:
  - Geometric lattice resonances with $|m_x|+|m_y| \leq 4$ mainly related to sextuples:
  $$m_x\nu_x + m_y\nu_y = \textbf{Integer}$$
  - Chromatic coupling resonances with $m_s = 1$ and 2 mainly related to nonlinear IR:
  $$\nu_x - \nu_y + m_s\nu_s = \textbf{Integer}$$
  - X-Z synchro-betatron resonances with $m_s = 1$ to 4 mainly related to dispersive sections (IR and Arcs) and beam-beam interaction:
  $$2\nu_x - m_s\nu_s = \textbf{Integer}$$
  - Y-Z synchro-betatron resonances mainly related to vertical impedances from small-gap collimators:
  $$2\nu_y - m_s\nu_s = \textbf{Integer}$$

- The most important beam-beam resonances with $m_y = 2$ and 4 due to large crossing angle and “hour-glass” effect:
$$\nu_x - m_y\nu_y + \alpha = \textbf{Integer}$$
- Here α is a parameter related to incoherent beam-beam tune shift and synchrotron tune.
- The resonance diagram with synchro-betatron resonances can be plotted:

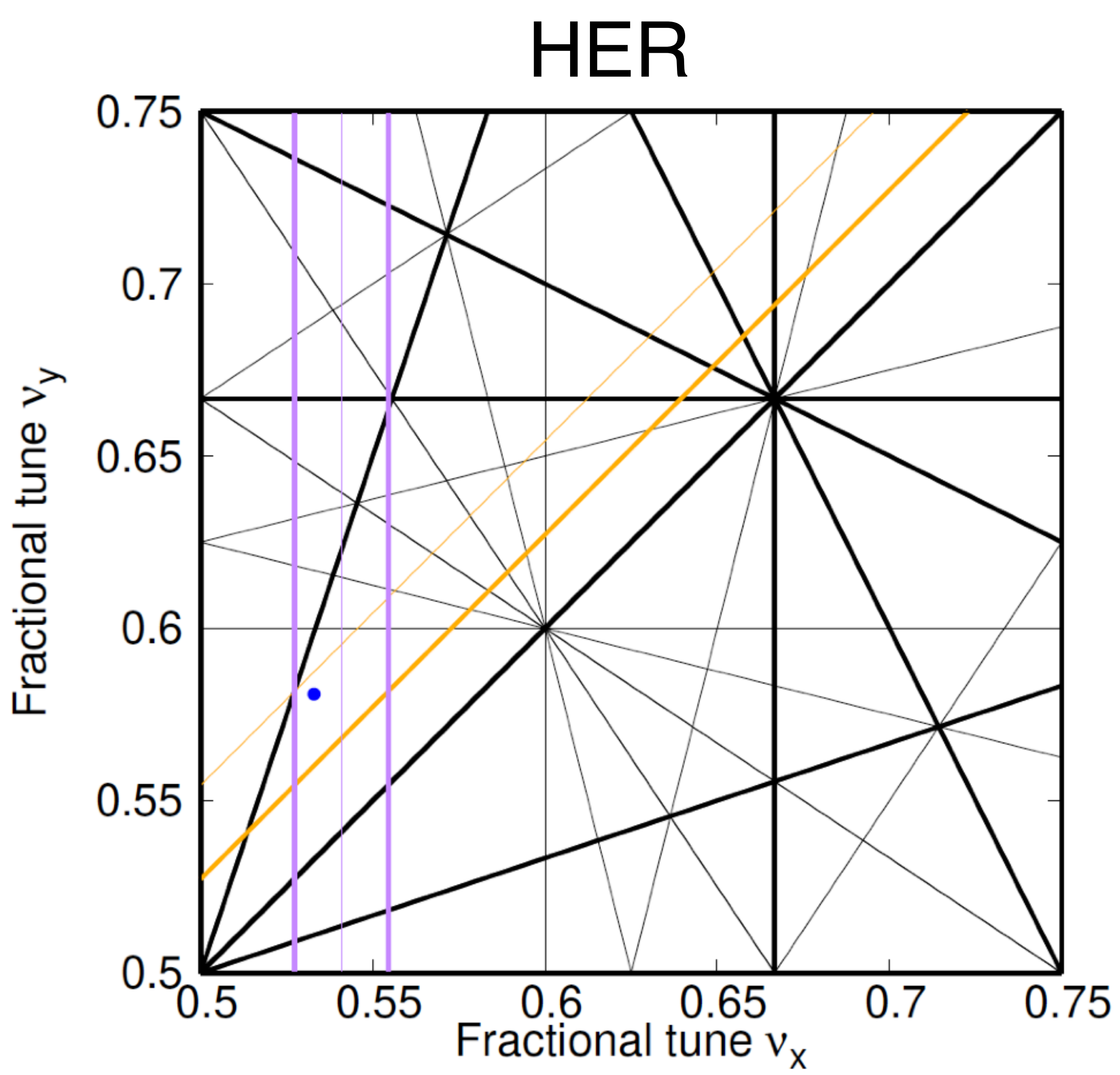

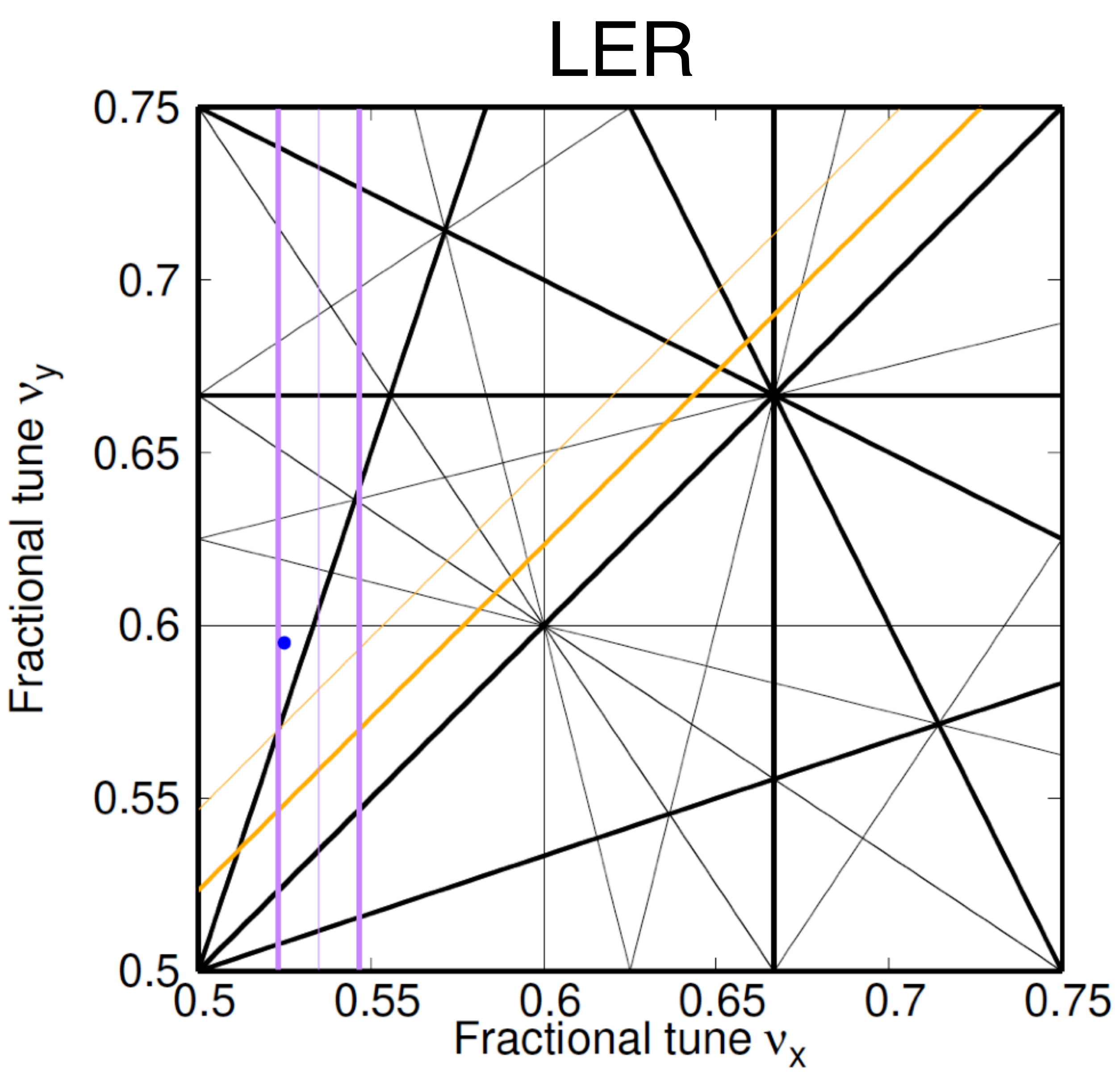

Interplay of beam-beam and lattice nonlinearity in SuperKEKB

- Using the resonance diagram for illustration: Beam-beam interaction and wake fields dynamic change the strengths, width and position of synchro-betatron resonance lines $m_x\nu_x + m_y\nu_y + m_s\nu_s =$ Integer. The footprint of the beam in tune space also depend on current and dynamically move around. It is difficult to locate the footprint in a region free from dangerous resonances.
- Crab waist is a key remedy, but achieving perfect crab waist is a new challenge.

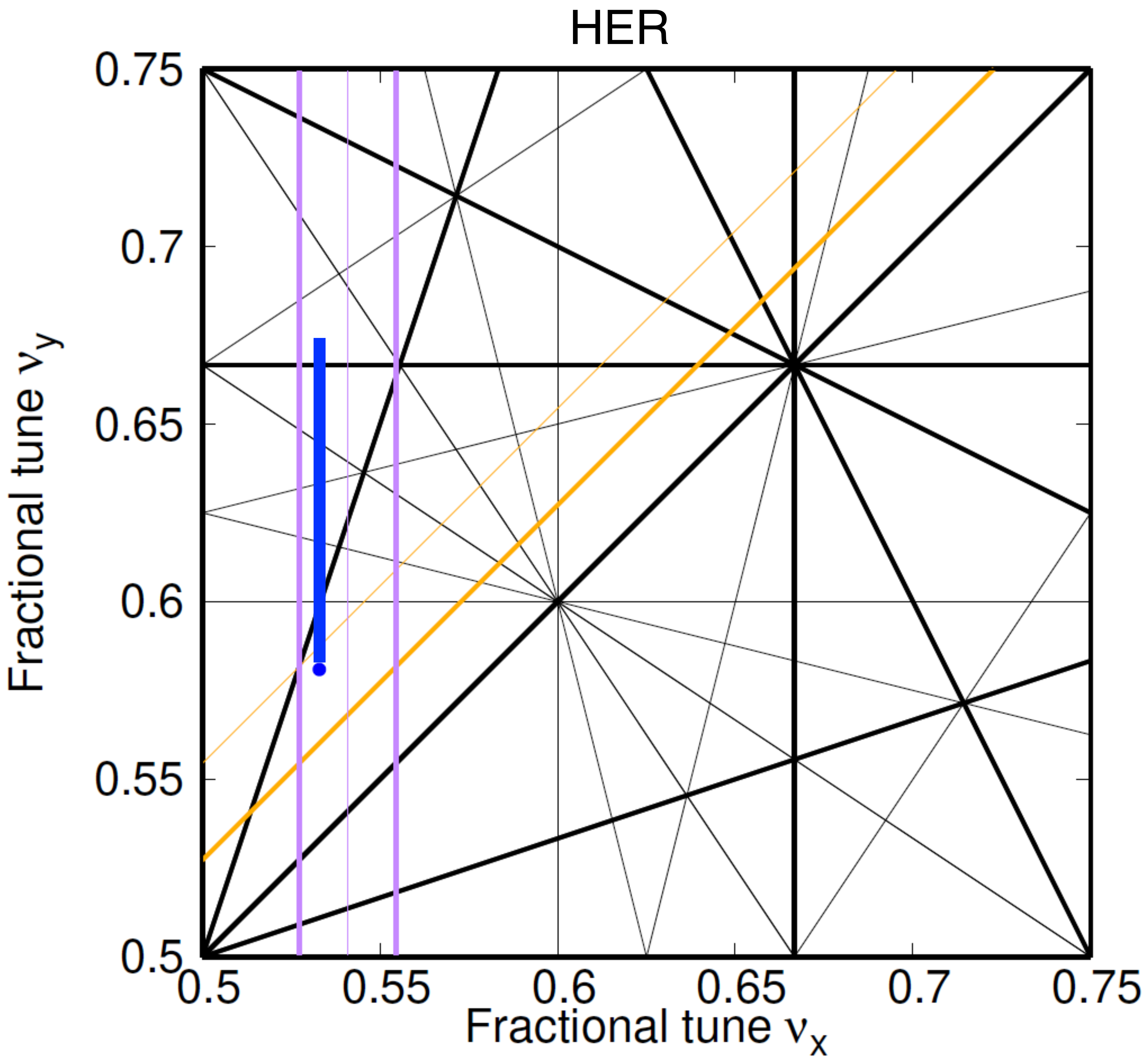

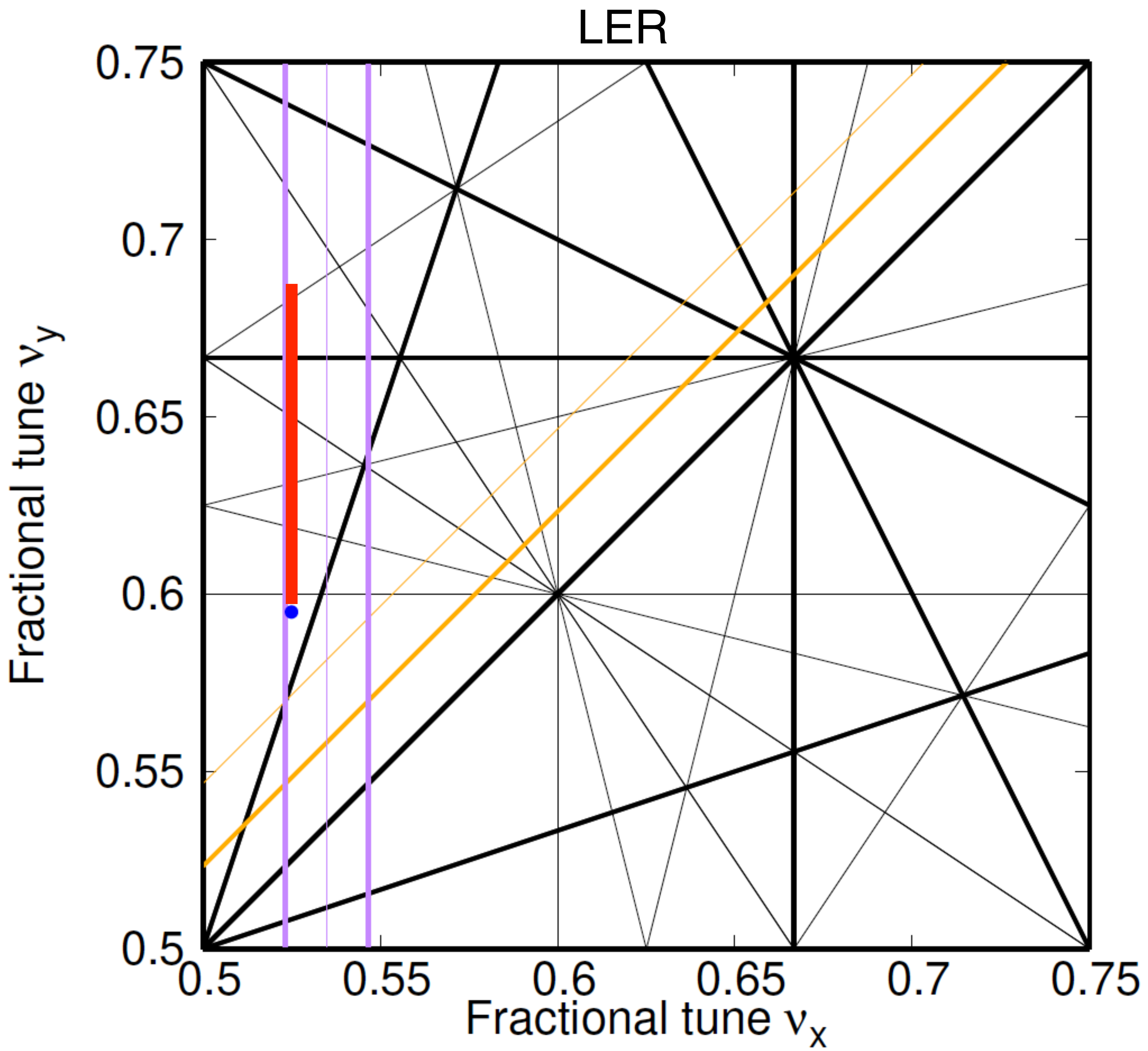

Interplay of beam-beam and lattice nonlinearity in SuperKEKB

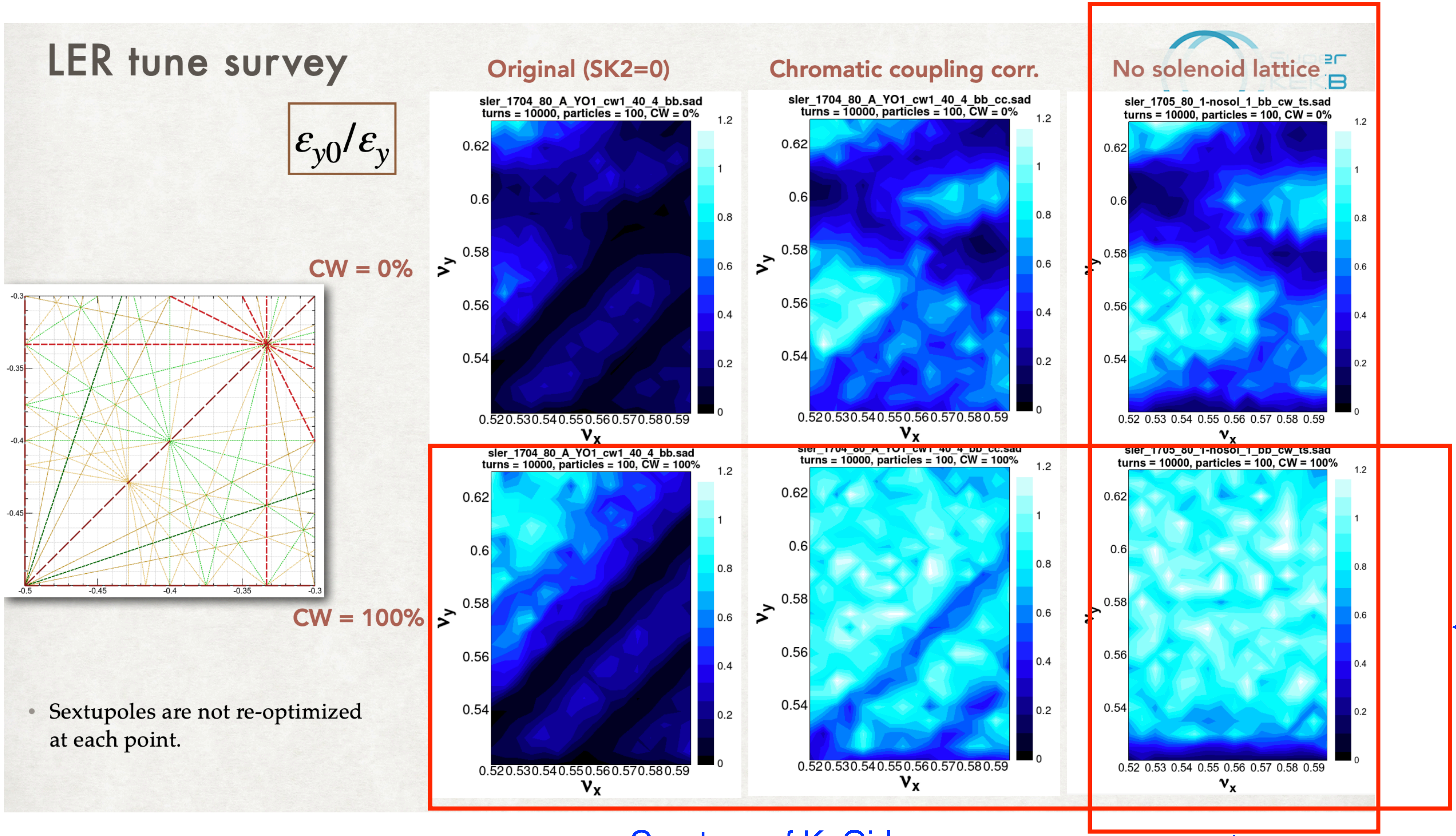

Crab waist

Courtesy of K. Oide

"Clean IR"

[1] K. Oide, https://kds.kek.jp/event/44644/.

"Clean IR": A transparent IR with minimal amplitude-dependent and chromatic nonlinearities

Summary

- A brief introduction to transfer maps and codes for accelerator modeling.
- Practical examples of transfer maps and their potential impacts on beam physics in SuperKEKB were discussed.
- An elementary introduction to converting transfer maps to nonlinear analysis was presented.

Backup

Single-particle linear dynamics

- Charge-particles' motion in electromagnetic field is governed by Lorentz force law:

$$\vec{F} = q(\vec{E} + \vec{v} \times \vec{B})$$

- In a uniform magnetic field a charged-particle takes circular motion [1].

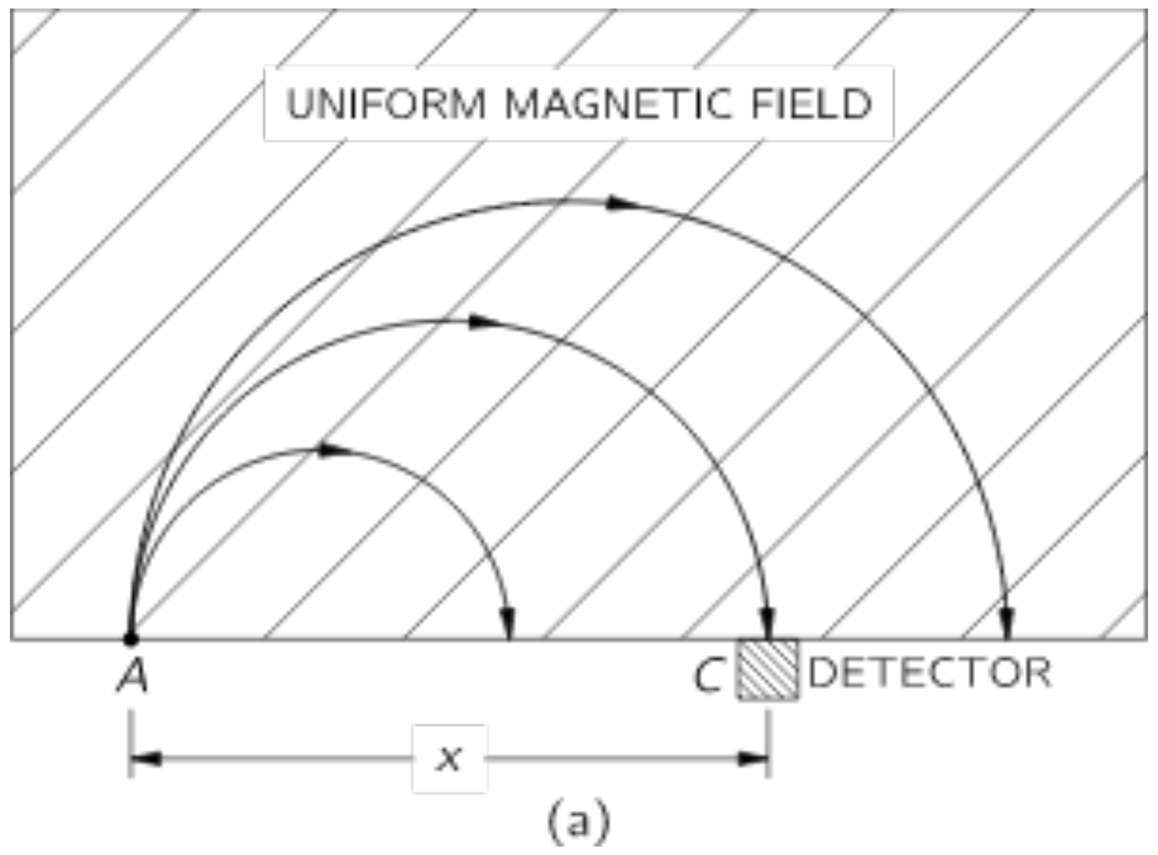

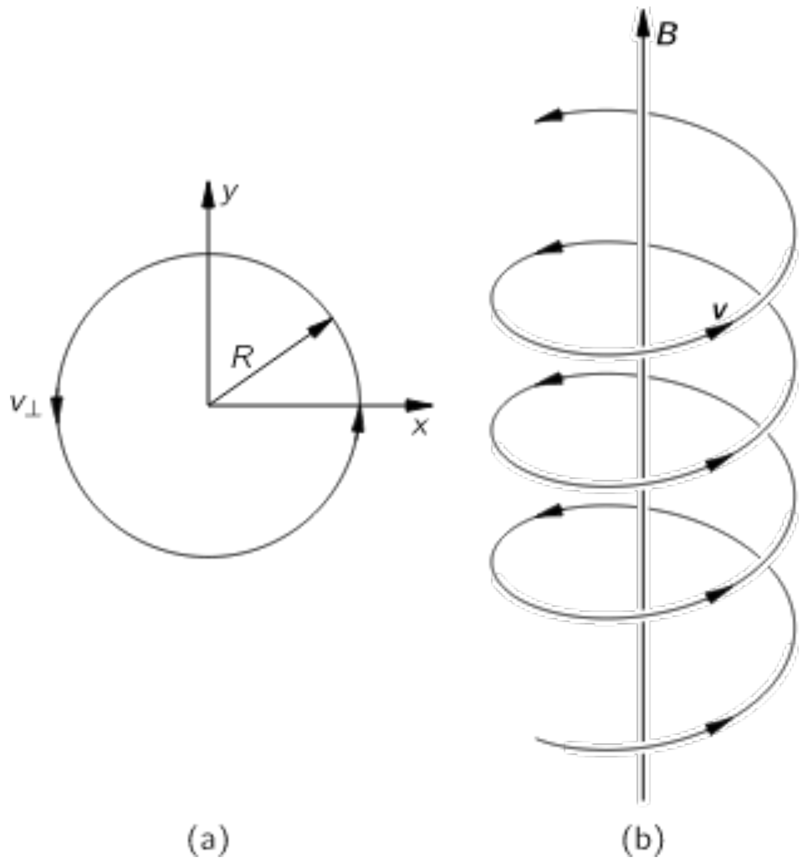

- Dipole magnets are used to create a circular particle accelerator. The beam circulates along a closed orbit ("Fixed point"): The particle trajectory closes on itself after one turn.

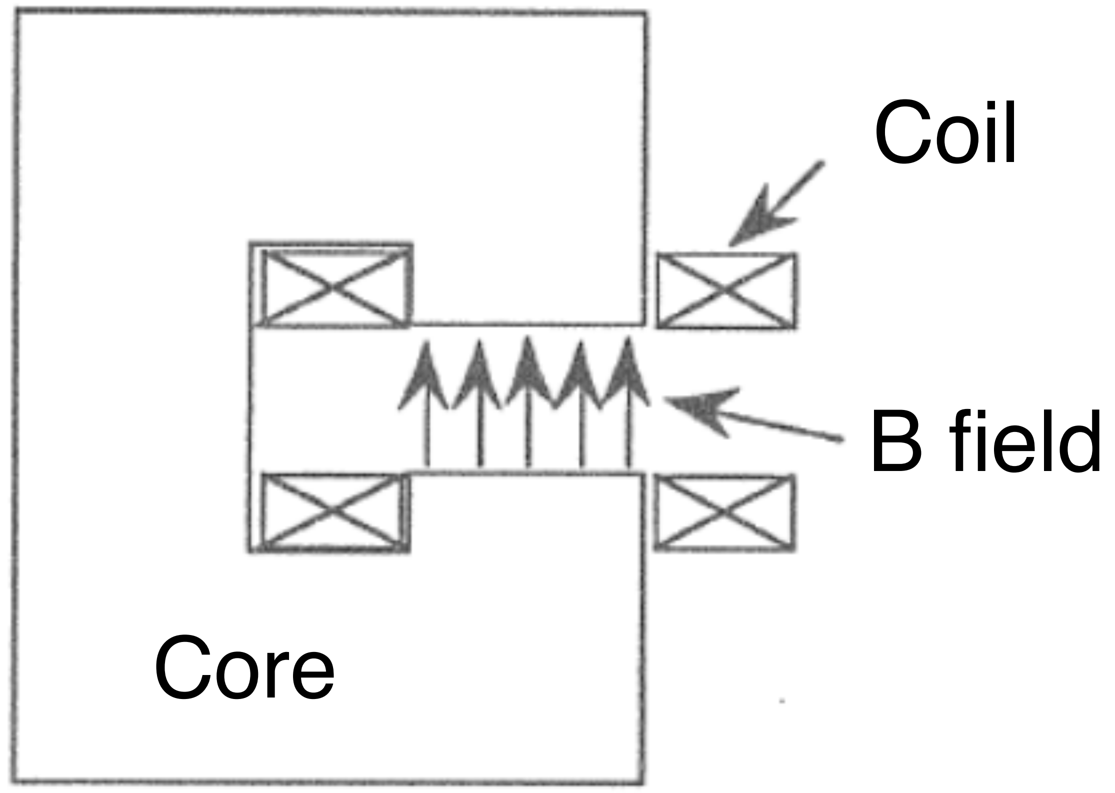

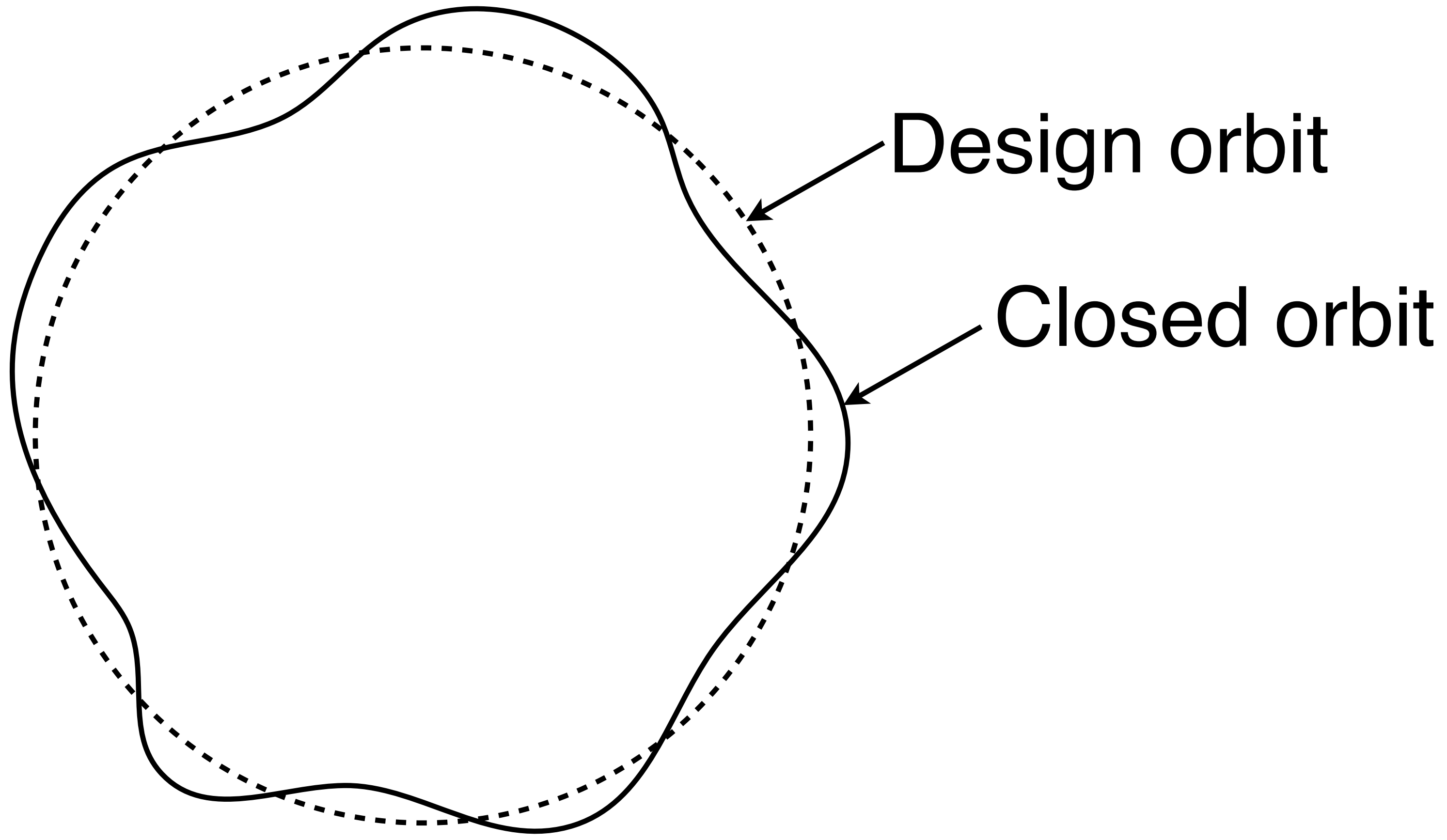

[1] R. Feynman, "The Feynman Lectures on Physics", https://www.feynmanlectures.caltech.edu/

Beam-beam perspective on achieving target luminosity

- How to achieve a "clean IR"
  - IR remodeling (the mainstream upgrade plan (see M. Masuzawa's talk) under investigation)
  - Using CCT (Canted Cosine Theta) magnets: M. Koratzinos did the first exercise (considering constraints from the technology and infrastructure of SuperKEKB) and showed encouraging results. Using the CCT magnets, a compact and cleaner IR is conceivable (Idea: "The current distribution of any canted layer generates a pure harmonic field as well as a solenoid that can be canceled with a similar but oppositely canted layer." [2]).

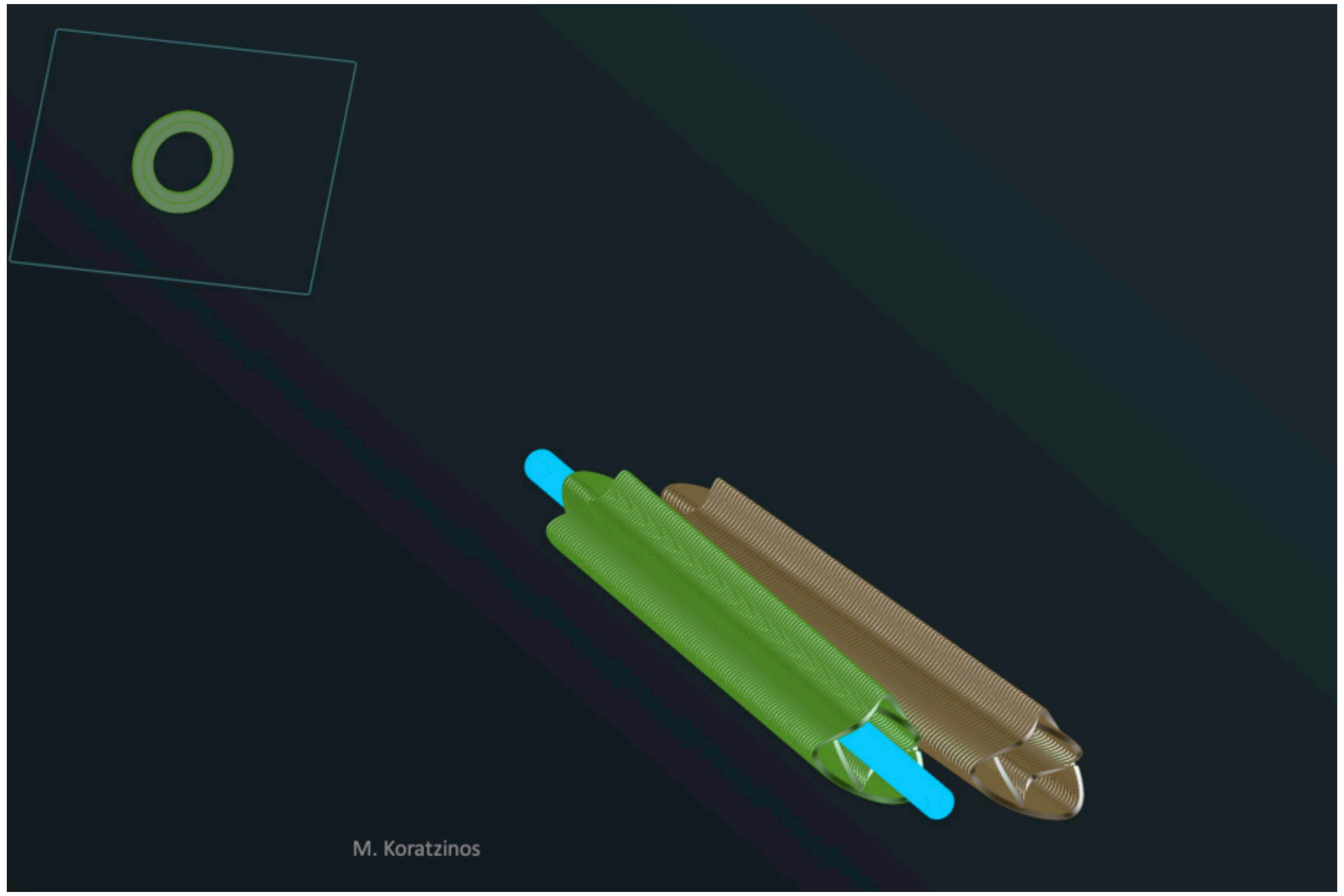

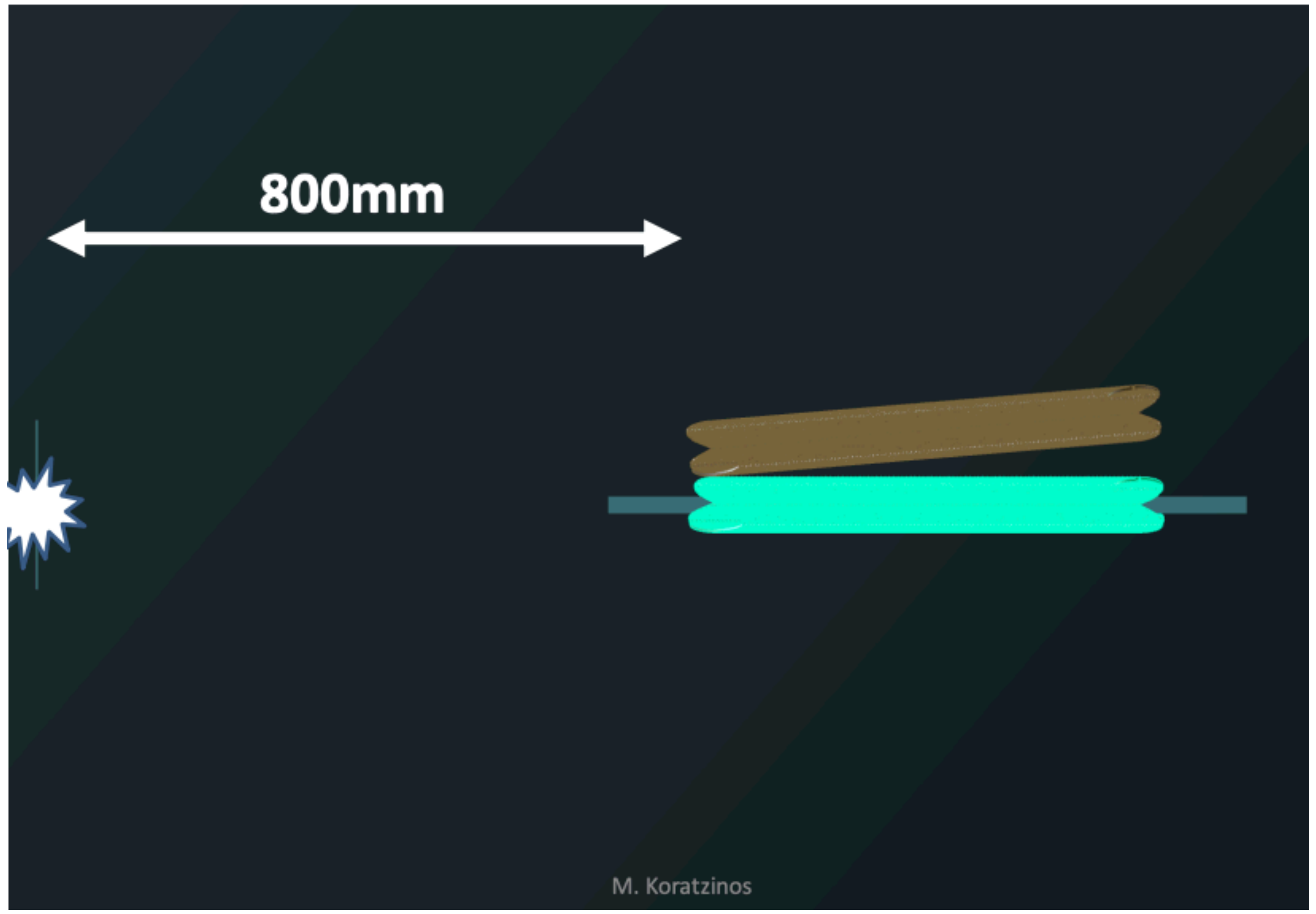

Courtesy of M. Koratzinos

  - From the beam-beam perspective, we invite full international collaboration on IR upgrades to achieve the target luminosity of SuperKEKB.

[1] M. Koratzinos, https://kds.kek.jp/event/44644/. [2] S. Caspi et al., "Canted-Cosine-Theta magnet (CCT)-A concept for high field accelerator magnets" , IEEE Trans. Appl. Supercond. 24, 1. (2014).